ISSN 0038-531X

Russian Original Vol. 57, No. 5, November, 1984

May, 1985

LL
JoT
JAL
File

SATEAZ 57(5) 751-802 (1984)

SOVIET ATOMIC ENERGY

АТОМНАЯ ЭНЕРГИЯ
(ATOMNAYA ÉNERGIYA)

TRANSLATED FROM RUSSIAN

c/b CONSULTANTS BUREAU, NEW YORK

SOVIET ATOMIC ENERGY

Soviet Atomic Energy is abstracted or indexed in *Chemical Abstracts, Chemical Titles, Pollution Abstracts, Science Research Abstracts, Parts A and B, Safety Science Abstracts Journal, Current Contents, Energy Research Abstracts,* and *Engineering Index.*

Mailed in the USA by Publications Expediting, Inc., 200 Meacham Avenue, Elmont, NY 11003.

POSTMASTER: Send address changes to *Soviet Atomic Energy,* Plenum Publishing Corporation, 233 Spring Street, New York, NY 10013.

Soviet Atomic Energy is a translation of *Atomnaya Energiya,* a publication of the Academy of Sciences of the USSR.

An agreement with the Copyright Agency of the USSR (VAAP) makes available both advance copies of the Russian journal and original glossy photographs and artwork. This serves to decrease the necessary time lag between publication of the original and publication of the translation and helps to improve the quality of the latter. The translation began with the first issue of the Russian journal.

Consultants Bureau journals appear about six months after the publication of the original Russian issue. For bibliographic accuracy, the English issue published by Consultants Bureau carries the same number and date as the original Russian from which it was translated. For example, a Russian issue published in December will appear in a Consultants Bureau English translation about the following June, but the translation issue will carry the December date. When ordering any volume or particular issue of a Consultants Bureau journal, please specify the date and, where applicable, the volume and issue numbers of the original Russian. The material you will receive will be a translation of that Russian volume or issue.

Subscription (2 volumes per year)
Vols. 56 & 57: $560 (domestic), $621 (foreign)
Vols. 58 & 59: $645 (domestic), $715 (foreign)
Single Issue: $100
Single Article: $8.50

CONSULTANTS BUREAU, NEW YORK AND LONDON

c/b
233 Spring Street
New York, New York 10013

Published monthly. Second-class postage paid at Jamaica, New York 11431.

SOVIET ATOMIC ENERGY

A translation of *Atomnaya Énergiya*

May, 1985

Volume 57, Number 5 November, 1984

CONTENTS

The Russian press date (podpisano k pechati) of this issue was 10/30/1984. Publication therefore did not occur prior to this date, but must be assumed to have taken place reasonably soon thereafter.

PROMISING ROLE OF NUCLEAR POWER IN AN ORGANIC-FUEL ECONOMY

S. Ya. Chernavskii

UDC 621.039

At the present time the problems of energy conservation stand out sharply. The developed industrial countries have for a long time satisfied an appreciable part of their energy needs by increasing the import of cheap oil. Having developed thus for several decades and having favorable long-term predictions of the world price of oil, they created a structure of consumption and production adequate for a low level of the world oil price.

As is well known, the sharp increase in the world price for oil in 1974 was not predicted. The energy crisis situation arose. Of course, at the time of the price jump nothing fundamentally new truly occurred in power engineering: the technical conditions of extraction and the predicted estimates of the energy reserves did not change, no new heavy power consumers arose, and no dramatic events took place in the field of energy conversion. The price jump denoted something different — the mechanism of distributing the profits was sharply altered. Under the influence of this new mechanism the oil-importing countries should have brought their consumption and production into agreement with the new price level. Since it is impossible to rapidly make the desired changes (power engineering is an inertial system), a nonequilibrium situation arose. For almost ten years we have been witnesses to the occurrence of nonequilibrium economic processes, whose goal is to adapt the production and consumption of energy, the entire economic system, and even lifestyle to expensive energy.

The changes have affected not only the importing nations but also our country. The intensity and content of adaptive processes are different in different countries. In some countries only power engineering has been adapted, and in others more general spheres have been subjected to action: economics and even social relationships. The economics and social structure of each country reacted to the energy crisis in a complex of measures, which one can divide into two groups. Measures to reduce the energy consumption levels make up one group. Here one can point out the exposure of unproductive losses and any kind of energy waste. One can call this kind of measure reversible. It should be said that one can bring some reversible measures into action rapidly; however, their role in the overall transition process to a new equilibrium state is evidently relatively small.

Measures which one can call intensive make up the other group. They are more significant in the first place in the long-term outlook. Among this group one finds in particular:

readjustment of the structure of energy consumers in the direction of a transition to a consumption technology which requires smaller consumption of the more expensive kinds of energy;

readjustment of the structure of extraction of primary energy resources, primarily by means of drawing new sources, including nuclear, into power engineering;

readjustment of the structure of electric power stations and heat recovery sources in the direction of the replacement of expensive fuel with cheaper fuel.

The time which is necessary to bring intensive measures into being is long; for some measures it amounts to decades. Therefore, at present the power engineering of the majority of countries is still in a process of adaptation to the high costs for oil and natural gas.

The growth in the world oil price fundamentally altered the economic estimation of all the main energy reserves of our country. The fraction which the export of energy resources is of their overall production has risen: in 1970 it amounted to 13%, and in 1980 — 17% [1]. The export of coal was stable and that of natural gas and electric power was small. Oil and petroleum products made up most of the export. The increasing efficiency of the

Translated from Atomnaya Énergiya, Vol. 57, No. 5, pp. 328-336, November, 1984. Original article submitted February 27, 1984.

0038-531X/84/5705-0751$08.50

bles/ton of conventional fuel

Region	Coal		Gas		Oil		Electrical power	
	1974	1979	1974	1979	1974	1979	1974	1979
Northwest	19	37	22	43	29	90	12	14
Center	18	36	22	42	29	90	11	14
Ukraine	19	35	22	45	29	90	12	14
Povolzhe	17	32	20	39	26	88	11	14
Ural	14	28	18	36	23	88	10	13
Central Siberia	6-8	8-10	14-16	28-30	19	85	7	10

export of energy resources caused an increase in the closing expenditures for fuel. Data on regions of the country obtained by the same procedure with an interval of 5 years are given in Table 1 [1].

The 1974 estimates reflect the state prior to the energy crisis, since up to this time no adaptive processes had yet been developed in power engineering.

It follows from Table 1 that the expenditures for coal and gas increased by a factor of two, for oil by a factor of three, and for electric power by 15-25%. Although at present the world oil price has decreased somewhat, the closing expenditures for fuel in our country have still not reached an equilibrium level, and one can expect the outlook to be for a further increase in them for some period of time.

One should note that the closing expenditures for electric power have not increased as appreciably as have the expenditures for fuel, mainly owing to the widespread use of nuclear energy. The development of nuclear power thus impedes a more rapid growth of the expenditures for organic fuel. An important problem is to clarify to what extent nuclear power can affect the consumption of organic fuel. In order to answer this question, one needs to determine:

the acceptability of nuclear power technology;

the regions and scales of penetration of nuclear power technology in dynamics;

the structure of nuclear power and the disposition of nuclear power installations.

Prior to proceeding to a discussion of these questions, we shall make several general remarks about the role of scientific methods in prediction.

Of course, it would be remarkable if questions similar to those under discussion could be successfully resolved with the help of rigorous scientific procedures, for example, as in mathematics. However, this is impossible. Not only because the future will bring something new to life which was previously unknown but because the actual technology, in particular energy technology, has a wide spectrum of links and actions and cannot be objectively described by any one efficiency indicator. Therefore the actual solutions regarding the development or freezing of this or the other energy technology are always assumed and should be assumed on the basis of a multicriterion discussion of the technology in question. Contemporary science can only in rare cases help to work out rigorously justified solutions. In real life it is necessary to operate from general concepts, follow particular criteria, and then simply exercise the will. Energy science is thus not omnipotent. It is necessary to use scientific methods as far as this is possible, not ascribing anything to science beyond its actual possibilities. Not all specialists are in agreement with this approach. Some defend this position: in the final analysis one can express the significance of all the diverse indicators with the help of a single cumulative scalar indicator (for example, discounted expenditures or usefulness), and others assert on the contrary that this makes no sense, because one can interpret discounted expenditures only with account taken of the economic structure in which they are calculated, because they assume usefulness to be too subjective a characteristic on which one could expect to operate. The viewpoint of the author consists of the fact that it is necessary in an applied prediction problem to make

use of the most completely scientific procedures, supplementing them with subjective estimates where this is unavoidable.

Now we shall return to the questions.

Acceptability of Nuclear Power Technology. The question "Is nuclear power acceptable?" has accompanied its development from the start of introduction of commercial nuclear power plants into operation. As is well known, the plans for development of nuclear power have encountered opposition on the part of some groups and population segments of such countries as the USA, West Germany, Sweden, and Austria. And now the solution of the problem of attaining a favorable attitude of these population groups to nuclear power has real value.

But what does the concept "acceptability" mean?

It is necessary here to distinguish two aspects: one is acceptability as an attitude (subjective) indicator to nuclear power, and the other is acceptability as correspondence to the interests or goals of a given individual, group, or population segment. Is is understood that the question of acceptability is resolved as a function of the specific situation. In different countries the mechanism of formation of an attitude of acceptability is different. For example, in Japan on the one hand the stockholders of a firm manufacturing nuclear reactors were interested in the development of nuclear power, since this increases the value of their shares, and on the other hand the consumers of electric power who live, let us say, not far from the nuclear power plant and do not have shares in the nuclear power firms relate positively to a reduction in the cost of electric power which they use, but this cost is not the main item in their budgetary expenditures. Therefore naturally other interests can be advanced to the forefront for such groups, for example, a reluctance to think about the possible danger of being located next to a nuclear power plant etc.

In our country there is no private ownership of the means of production, and there are no shareholders. At the same time a mechanism operates for the adoption of planning solutions which is oriented to a large extent to bringing into existence measures which would correspond to State interests. Therefore the question of acceptability acquires an important aspect: how to find solutions which would correspond to the greatest extent both to the general and to group and personal interests.

The question of the economic side of acceptability is a traditional one, but as formerly, one of the most important. More will be said about it later, but now we shall consider a little-studied aspect — the psychological.

A study of public opinion carried out at the Center of Nuclear Research at Jülich (West Germany) has shown that nuclear power is estimated by the population as the most economical kind of technology in comparison with another, for example, solar or coal [2]. However, it is estimated at the same time to be the least attractive. Where do you suppose such notions come from? In fact numerous papers of specialists have shown that if one takes account of all the direct and indirect costs associated with the development of this technology, it is precisely nuclear power which turns out to be the safest. Why does part of the population not accept the viewpoint of the majority of the specialists but regards it at least with suspicion? The answers to these questions, which are important for evaluating the outlook for nuclear power, lie in the psychology of the individual.

O. Cohen, explaining the phenomenon of negative attitude towards nuclear power [3], assumes that one of the most important factors responsible for this phenomenon is the absence of familiarity with nuclear power technology, which has still not been integrated into the way of life. He notes that mankind has developed over an extended time, extracting energy from organic fuel, and has had time to become familiar with this technology. But nuclear power is a new technology to which familiarity has not yet developed. Cohen and other authors assume that as time goes on experience with the safe operation of nuclear power plants will result in development of the necessary familiarity on the part of those who now regard nuclear power negatively.

But the matter, however, is somewhat more complicated. Of course, familiarity is an important psychological factor when one is talking about acceptability. However, people have also not yet had time to become accustomed to solar power, and it has been shown in the investigations mentioned that solar power is estimated to be the safest and most attractive. Thus the matter is not just one of familiarity with the technology as much as it is one of

the existence of a psychological mechanism of the transfer of an attitude from one phenomenon to another. The positive attitude towards the Sun is transferred to the attitude towards solar power. On the contrary, its wartime use preceded the use of atomic energy for peaceful aims. The atomic bomb explosions at Hiroshima and Nagasaki as well as the development of even more powerful atomic, hydrogen, and neutron weapons are linked in the consciousness and subconsciousness of many people with the subsequent process of development of nuclear power. Thus a negative attitude towards nuclear weaponry can be transferred with the help of a psychological mechanism to nuclear power.

The specific nature of the action of nuclear power on the environment also exerts an effect on the formation of a negative attitude towards it on the part of a segment of the population. We are talking about ionizing radiation. Its peculiarity lies in the fact that it is not sensed by an individual but can be potentially dangerous. Thus nuclear power creates a special psychological atmosphere for those who, in particular, live near the locations of nuclear power facilities. This atmosphere is related to that which is created in the cabin of a passenger airliner. As is well known, some passengers experience discomfort from the fact that their safety is in the hands of other people, in this case the airplane pilots. The pilots themselves have no sense of anxiety. This is understandable — in fact they control the airplane. It is also well known that not all the passengers of airplanes experience a sensation of discomfort in flight.

One can assume that some of those who live near nuclear power installations will continually experience discomfort. The consequences of an extended stay in a state of discomfort are not clear. It will possibly be necessary to adopt special measures to compensate for this "psychological contamination" of the environment by nuclear power. Taking account of the psychological contamination of the environment by nuclear power should increase somewhat the expenditures for development of this technology, but what is more important, it can influence the optimal solutions.

One more factor of psychological contamination is associated with incidents at nuclear power installations. Great significance has always been attached to the prevention of accidents at nuclear reactors. As a result traditional power technology is appreciably inferior to nuclear power in its ability to withstand accident situations. The incident at the Three-Mile Island nuclear power plant (USA) has convincingly demonstrated this. However, it revealed the appreciable psychological action of such incidents. One can conclude from this that is is exceedingly important for the accelerated development of nuclear power not to allow accidents to occur, all the more with heavy consequences. It is evidently advisable to expend part of the economic efficiency reserve of nuclear power on the adoption of additional measures whose aim is not to allow psychological contamination by it of the environment.

Concluding the discussion of the question of the acceptability of nuclear power technology, one can say that in order to increase the degree of acceptability of nuclear power it is necessary to expend additional means. It is still not clear in my opinion what the consequences will be of the placement of some kinds of nuclear power installations, in particular atomic reactors, in direct proximity to populated sites or even on their territory. This is evidently advisable in the later stages of development of nuclear power when the horror of psychological contamination on its part has significantly subsided.

Regions and Scales of Penetration of Nuclear Power Technology. The traditional region of penetration of nuclear power is electric power just now. Other areas, primarily central heat supply both of low and high potential, are discussed for perspective. The possible scale of penetration of nuclear power into these spheres depends on the technical utilization and economic indicators of nuclear power installations.

One should bear in mind that contemporary nuclear power plants produce not only electric power but also heat in the form of hot water for intrinsic needs and for living quarters. However, the fraction of the energy produced in the form of heat is inappreciable in the schemes of nuclear power plants. Therefore they are of the condensation type. One can assume that up to now nuclear power has been producing energy in the form of electric power. In 1980 $\sim$ 400 million tons of conventional fuel was expended for the production of electric power and $\sim$ 500 million tons of conventional fuel was expended for low-temperature heat, which corresponds to 22 and 26% of the total consumption of energy resources for the internal needs of the country. In 1980 nuclear power plants produced 73 billion kWh of electric power [1]. The specific consumption of fuel at plants burning organic fuel amounted to 328 g of conventional fuel/kWh. Thus the development of nuclear power just for the production of

electric power has permitted saving 24 million tons of conventional organic fuel, or about 6% of the total amount of fuel expended for the production of electric power. Of course, this is still not very much. However, it is important to note that until now petroleum residue has been consumed in our country for the production of basic electric power; therefore one can attribute the estimate obtained to a savings of expensive petroleum residue. With account taken of this understanding of the role of nuclear power in an organic fuel economy, one can now uncouple its contribution as an appreciable one.

There are no doubts that nuclear power will increase its contribution in the future to the production of electric power in our country. However, on the agenda is the industrial utilization of atomic central heating power plants (ACHPP) and nuclear heat supply plants for the production of hot water. In the more distant future one can expect the use of atomic energy to produce high-potential heat. We will yet return to a discussion of these questions, but just now we shall discuss in more detail the conditions of development of nuclear power in electric power engineering.

In the first approximation one can consider the economic indicators to be independent of the location of nuclear power plants. Strictly speaking, this is not so, since the conditions of construction of nuclear power plants differ by regions of the country; for example, they are different for the European and Asian parts, especially for those regions in which the climate is more severe. Concerning the fuel component, it can be assumed to be constant for nuclear power plants for the entire territory of the country. Although the conditions of the water supply in different regions of the country are different, which affects the cost of construction, however, for the large regions united within the framework of a single combined energy system, one can at the present time almost always find those small areas* for which the cost of water supply will not be too high. Only certain regions of Middle Asia and the Ukraine, where the water balance is strained, comprise an exception.

The cost of construction of power stations using organic fuel (thermal electric power plants — TEPP) can also be assumed to be independent of their location, but on the contrary location has an appreciable effect on fuel cost (see Table 1). Such a dependence is truly significant only when one is talking about coal-fired power plants, since their economic indicators depend to a greater extent on their distance from a coal basin. The indicators of power plants using natural gas suffer to a lesser extent from the cost of transportation. Concerning the cost of petroleum residue, its transportation is inexpensive.

Thus the competition conditions between nuclear and thermal power plants will be different in regions of the country located in proximity to deposits of cheap coal (this is primarily the region of Central Siberia and the Kuznetskii and Kansko-Achinskii Basins) and in regions located far from deposits of cheap coal (this is primarily the European part).

As is well known, a plot of the consumption of electric power is a nonequilibrium one, and this nonequilibrium creates specific competition conditions between nuclear and thermal power plants, since investments play the greatest role in the cost of nuclear power plants, and fuel cost plays the same part for thermal power plants located far from coal basins.

First we shall give a predictive estimate of the specific investments. First of all it is necessary to note the unsatisfactory nature of the direct use of design estimates as predictive ones. Of course, the design data of power plants are important; it is necessary to take them into account in prediction, but it is impossible in the majority of cases to convert them into a prediction without any corrections, since this will result in incorrect results. It is generally known that the actual values of the investments exceed in the overwhelming majority of cases the design indicators. There are many causes for this. One of them is that it has not proven possible in the design especially of nuclear power plants, for which there is still little experience, to reveal opportunely all the difficulties which will appear in the course of the construction and the operating process. Overcoming problems which arise requires additional expenditures of time and materials. To a definite extent making designs less expensive is stimulated by the labor estimation method of the designer. Of course, the designer is interested in presenting his best work. An important factor which leads to a reduction of design values is to estimate in the design the cost of the resources used not according to the closing costs but according to the mean branch costs

*This is valid, of course, for small scales of development of nuclear power. They will cost more in the prospect for a small area due to a deficit of natural resources (water, ground, etc.).

TABLE 2. Correction factor β_i to the design specific investments, %

Factor	Thermal power plants	Nuclear power plants
Changes introduced in the course of construction due to the appearance of unexpected difficulties, the appearance in the course of design of a tendency to present his own project better, and also stimulation of the designers to make the design less expensive	3-9	7-17
Estimate of the cost of materials and labor not according to the closing but according to the accounting costs compiled on the basis of the average expenditures	10-17	13-20
Changes introduced in the course of the construction due to increased costs of materials and equipment upon converting from calculations using prime cost to reduced costs	0-3	0-5
Total	13-29	20-42

(it is precisely the latter which lie at the basis of the accounting costs which are used in the design). Sometimes they also do not take account of the fact that development requires the construction of new undertakings servicing the power industry. The cost of their production will be higher than the current costs, which are established on the basis of the concept of prime cost, especially when production is furnished from plants constructed long ago.

Is is clear from what has been said that the specific investments in new power facilities calculated on the basis of design estimates can be calculated using the formula

$$K = K_d\ (1 + \sum_i \beta_i/100)\,\beta_c, \tag{1}$$

where K_d are the design estimates of investments not discounted during the years of construction, β_c is a coefficient which takes account of the discount during the construction years, and β_i is a correcting factor which takes account of the role of the i-th factor of those about which we have talked, in %.

The coefficient β_c is calculated from the formula

$$\beta_c = 1/t_c \sum_{t=-(t_c-1)}^{0} (1+\sigma)^{-t}, \tag{2}$$

where σ is the discount coefficient and t_c is the construction term in years. A uniform distribution of investments over the construction years has been assumed. According to Eq. (2), the specific investments are reduced to the year in which the construction is concluded. Concerning the values of β_i, there should be a clear understanding of the fact that it is necessary in the design to deal with subjective estimates and that this coefficient is just an example of these kinds of estimates.

The author's estimate of factors which reduce the design values in comparison with the actual ones for nuclear and thermal power plants is given in Table 2. The TEPP are in the form of power plants in which basic coal-fired units are located, and the nuclear power plants are ones with thermal reactors. This table is essentially subjective and does not exclude other representations.

We shall adopt the following values as the initial estimates of K_d: for thermal power plants — 170 rubles/kW, and for nuclear power plants — 270 rubles /kW [4]. Then using the

data of Table 2, we obtain an estimate of the investments which are still not discounted for the construction period. They will amount to 190-220 rubles/kW for thermal power plants and 320-380 rubles/kW for nuclear power plants.

A question which is important for prediction is how will the specific investments vary in the future. They will evidently be under the influence of both raising and lowering factors.

In the first place, as society continues to develop on the one hand a widescale penetration of power engineering, and consequently an intensification of the action on the environment on the other hand, the requirements being imposed on the power facilities, in part a provision for their greater safety and the localization of harmful wastes, will increase. One can observe this process already today when people talk about the necessity of switching to closed water supply systems for power plants, the installation of wet scrubbers at coal-fired thermal power plants for sulfur removal, systems for localization of the maximum accidents at nuclear reactors, and so on. The satisfaction of such requirements raises the investments.

Secondly, as time passes the cost increases due to the increase in cost of the ground made unavailable under the power plant; in addition it is necessary to build the power plants themselves on more expensive plots. The outlook is for the value of the natural (intrinsic) surroundings to increase. Thirdly, as more and more volumes of material resources are drawn into economic activity, the closing costs for raw materials and labor will grow. One of the causes for the increase in the cost of nuclear power plants is a tendency to greater automation of the operating process.

Finally, factors which reduce the investments also act in time. This is primarily the improvement of the technology, which is observed not only in power engineering but also in related fields.

Thus an estimate of the specific investments for year t of the prediction period can be made using the formula

$$K_t = K\left(1 + \sum_j \beta_j^t/100\right)\beta_c^t/\beta_c, \tag{3}$$

where K are the specific investments determined using formula (1), β_c is a coefficient determined using formula (2), and the subscript "t" indicates that the corresponding parameter pertains to the year t.

TABLE 3. Correction Coefficient β_j^t, %

Factor	10 years		30 years	
	thermal power plant	nuclear power plants	thermal power plants	nuclear power plants
Increase in the unit power of an energy unit and improvement of the construction	−(2—4)	−(6—8)	−(2—4)	−(7—10)
Increase in the capacity of the power plant	−(2—5)	−(3—7)	−(2—5)	−(3—12)
Improvement of fabrication and construction	−(1—2)	−(2—4)	−(1—2)	−(3—5)
Increase in the requirements on power facilities	+(2—5)	+(4—10)	+(3—7)	+(6—12)
Increase in the closing costs for materials and labor	+(2—10)	+(2—10)	+(4—14)	+(4—16)
Deterioration of the quality of small areas	+(0—2)	+(0—2)	+(3—6)	+(4—8)
Total	−1 ÷ +6	−5 ÷ +3	+5 ÷ +16	+1 ÷ +9

TABLE 4. Estimate of the Specific Investments for Different Points in Time, rubles/kW

Investments	Depth of the prediction years		
	0	10	30
Undiscounted for the construction period at:			
thermal power plants	190—220	185—235	200—255
nuclear power plants	320—380	305—390	325—415
Discounted for the construction period at:			
thermal power plants	255—295	250—315	270—345
nuclear power plants	495—585	440—560	415—525

The author's estimate for two points in time located 10 and 30 years from the start of the prediction period, respectively, is given in Table 3. On the whole it follows from this table that an increase in the specific investments in time is characteristic both for nuclear power plants and thermal power plants.

Here it is again appropriate to recall that the data presented in Table 3 reflect the subjective estimation process of the author. Other specialists involved in the prediction of the indicators may take a different position on this question.

The resultant estimates of the investments calculated using formulas (1) and (3) are presented in Table 4.

When estimating the fuel component of the cost of electric power, one should bear in mind that its share of the total production expenses of nuclear power plants is small. In the future this role will be smaller yet, provided there is widescale development of fast reactors. In addition the calculation of the fuel component for nuclear power plants can be done only within the framework of all of nuclear power.

Concerning the fuel component of the energy cost of thermal power plants, it plays a basic role in the cost structure. It is necessary when estimating the effectiveness of nuclear power to take account of the fact that at present a lot of petroleum residue and gas are being burned at power plants. Thus in 1981 the share of petroleum residue in the fuel structure amounted to 28.5% and that of natural gas — 21.6% at the Minénergo power plants of the USSR [5]. Thus coal and atomic energy will not compete in the next years until petroleum residue and then natural gas are forced out of the production sphere of basic electric power, but on the contrary they will serve in a common goal — to force petroleum residue and natural gas as a fuel out of the basic part of the electric load plot. The advisability of satisfying this problem is dictated by the high efficiency of the use of these energy resources in other spheres of the national economy and their trend for export.

Different viewpoints have been expressed in the literature on the question of the relationship between closing estimates for oil and the world price for oil. According to one of them, "the national economic estimate of exported liquid fuel is significantly lower than its world prices" [1]. The calculation given in the cited book gives an estimate of 55 rubles/ton of conventional fuel for oil in the case that the relationship of prices for imported and similar domestic equipment is equal to 0.5 and 112 rubles/ton of conventional fuel if the indicated relationship is equal to unity. It has been assumed by the author of the calculation that the export efficiency is calculated on the assumption of the use of an additional currency aid for the purchase of equipment for heavy industry.

There is another point of view, according to which the national economic estimate of petroleum residue and oil is close to the world prices. This point of view is justified by the fact that it is necessary when estimating the effectiveness of additional currency aid to proceed from the fact that other goods are imported along with equipment for heavy industry. As a calculation made by the author shows, oil should be estimated at 160 rubles/ton of conventional fuel with this assumption taken into account. At such a high price petroleum re-

TABLE 5. Estimate of the Costs for Production of the Basic Electric Power, kopecks/kWh

Indicator	0		10 years		30 years	
	thermal power plants	nuclear power plants	thermal power plants	nuclear power plants	thermal power plants	nuclear power plants
Number of hours of use of the capacity in a year, h/yr:						
7000	2,5—2,6	1,9—2,1	2,5—2,7	1,8—2,2	3—3,2	1,7—2,1
5000	2,8—3	2,5—2,9	2,8—3,1	2,4—3,0	3,3—3,6	2,3—2,8

sidue should be forced out as rapidly as possible from electric power and central heat supply as the main fuel. First of all, one can replace petroleum residue with natural gas at existing power plants, since the majority of the units in which petroleum residue is burned have a supply of gas. If one assumes that the expenditures associated with the construction of additional gas supplies and the equipping of additional gas reservoirs will amount to ∿ 15-20%, it turns out that the cost of natural gas will be equal to ∿ 120-130 rubles/ton of conventional fuel in the European part. Thus it is inadvisable to burn natural gas for the production of the basic electric power. Atomic energy and coal will compete only after petroleum residue and natural gas as a fuel, with whose help the basic electric power is being produced, are forced out.

What can one say about coal? If one talks about the European part, in our opinion this is the coal of the Kuznetskii Basin with a caloricity of ∿ 5300 kcal/kg. After some expenditures for enrichment the caloricity can be raised to ∿ 6200 kcal/kg. Railroad transportation is cheap, and the output conditions are such that labor productivity can be ensured, exceeding that achieved at Donbass — the main coal basin of the European part of the country — by a factor of two-three. An estimate of the reduced costs based on an estimate made by the author of the specific investments in power plants located in the European part of the country is given in Table 5. In the compilation of the table thermal power plants were understood to be ones operating on Kuznetskii coal.

It should be noted that the author's estimate diverges somewhat from those of other authors. Thus for power plants using Kuznetskii coal with 500-800 MW units (and this is the most promising unit capacity of coal-fired units) the reduced expenditures are estimated to be 1.46-1.54 kopecks/kW [1] upon the utilization of a thermal power plant for 6000 h/yr, 1.2-1.35 kopecks/kW for basic coal-fired thermal power plants in the Southwest, Central, and Southern regions [6], and 1.6 kopecks/kW for 5000 h/yr [4]. The reduced costs for nuclear power plants are equal to 1.94 kopecks/kW for 5000 h/yr [4] and 0.98-1.1 kopecks/kW [6].

The data of Table 5 convincingly show the economic advantages which the economy receives from placement of nuclear power plants in the European part of the country. Concerning the regions of Central Siberia, the construction of thermal power plants with boilers in which coal of the Kansko-Achinskii Basin is burned is more effective for the production of the basic electric power. This coal is brownish black with a caloricity of ∿ 3040 kcal/kg; it is most effective to use it in regions located not far from the extraction sites.

The possibility of the effective use of nuclear power plants with a specified reduction in the number of operating hours provides for their large economic reserve in the European part of the country. However, it should be kept in mind that these nuclear power plants are still not adapted to daily and weekly shutdowns, so that a reduction in the number of operating hours can be achieved only by decreasing the load of the units but not by a shutdown. According to the data of Table 5, nuclear power plants are more efficient in comparison with thermal power plants using Kuznetskii coal up to 5000-5500 operating hours per year but are less economical when there are less than 3500 operating hours per year.

An interesting question is what is the efficiency of central heating, in particular, using nuclear fuel. One can determine the role of central heating only by a combined discussion of the production of electric power and heat. Central heating is a traditional direction in the development of power engineering in our country. During the period of predominant use of organic fuel the construction of central heating power plants (CHPP) permits saving organic fuel in many cases, and when petroleum residue and natural gas were cheap, gas—petroleum residue CHPP, saving petroleum residue and gas, gave "clean" electric power and heat. Central

heating plants using natural gas are today appreciably better than CHPP using coal with respect to air pollution. However, with expensive petroleum residue and gas CHPP also prove to be an expensive technology for the production of basic electric power. It is true that CHPP calculated for covering the purely basic heating load evidently have some promising features. However, this load is small. And what is the possible role of nuclear central heating?

At present the economic indicators of ACHPP do not seem completely clear to the author. The reason for this indeterminateness is objective. If there is still little operating experience with nuclear power, there is almost none in the ACHPP field.

An important argument in favor of the development of ACHPP is that their construction will help free up not only expensive petroleum residue and gas but also the cheaper coal from the balance of the basic part of the heat production.

And what are the arguments against it? First of all, the requirements on ACHPP are more rigorous than on nuclear condensation power plants by virtue of their closer location to population centers. Satisfaction of these requirements makes the electric power produced by ACHPP more expensive. Secondly, ACHPP have the following inadequacy in comparison with CHPP — they locate them further from cities than CHPP using organic fuel, which requires additional hot water pipes 30-40 km in length. (It is true that the additional distance in the case of ACHPP has an important positive value. The time which the water takes to cover this distance is several hours; this is long enough that in an emergency situation it could be disconnected from the consumers.) In addition the probable placement zone of ACHPP is the suburban zone, which is, as a rule, a relaxation area for city dwellers. The cost of land in the suburban zone in high.

An ACHPP is a large producer of heat; however, the community everyday load even in areas of massive multistory construction is a concentrated one. Therefore a single reactor with a capacity of 1 million kW should evidently be standard equipment of an ACHPP. One should use other types of equipment, for example, gas boilers, as the reserve capacity. There is no need to locate the reserve boilers far from the city. Thus, the system of heat supply from ACHPP should be located on two plots, one of which is located far from the city, on which the nuclear reactor is located, and the other — in the city itself or in the direct vicinity of it. The reserve and peak boilers are located on this second small plot.

From the standpoint of the limited nature of resources of cheap natural uranium and the development of fast breeder reactors it seems more promising to have a separate setup for heat production in which the basic part of the heating load is satisfied by nuclear heat supply plants (NHSP) and the peak part is satisfied by boilers burning organic fuel. In the outlook for the future NHSP will be more economical sources of basic heat in comparison with

TABLE 6. Effectiveness of Penetration of Electric Power Based on Nuclear Power Plants in Comparison with the Direct Use of Organic Fuel

Cost of electric power based on nuclear power plants, kopecks/kW	Cost of organic fuel, rubles/ton of conventional fuel		
	60	150	200
Low-temperature processes:			
1,0	—	=	+
3,0	—	—	—
High-temperature processes:			
1,8	—	+	+
3,0	—	+	+

The symbols "+", "-", and "=" denote advantage, disadvantage, and equivalence, respectively.

boilers using natural gas, and they will not force fast breeder reactors out of the area of production of electric power. However, NHSP have still not been tested on a large scale, and the problem of their acceptability, which we spoke about earlier, has not yet been resolved.

In conclusion, one should dwell once more on one question. The economic reserve which nuclear condensation power plants have in comparison with a technology which uses organic fuel will facilitate further electrification of consumers and elimination of the consumption of organic fuel from technological processes. Taking account of the fact that the total expenditures (non-power) along with the capital component for electrical technology are, as a rule, equal or even higher than in connection with the direct burning of fuel, one should consider widescale electrification of technological processes as the most important measure facilitating the forcing of liquid and gaseous fuel out of internal energy consumption and lowering the national economic costs. It indicates that the replacement of liquid, and then gaseous, fuel by nuclear energy is economically advantageous for almost all consumers (large-scale) with a basic load. The electrification of high-temperature processes using nuclear power is the most effective. The advisability of the electrification of low-temperature processes depends to a large extent on the economic indicators of nuclear power plants. The data of Table 6 sheds some light on this matter.

The effect of the structure of nuclear power on the economic efficiency of the replacement of organic fuel by atomic energy has not been discussed in this paper. This question would require a special analysis and the discussion of a special methodology. One of the possible versions of such a methodology has been suggested in [7].

LITERATURE CITED

1. L. A. Melent'ev and A. A. Makarov (eds.), The Energy Complex of the USSR [in Russian], Ékonomika, Moscow (1983).
2. O. Renn, "Nuclear energy and the public: risk perception, attitudes and behavior. Uranium and nuclear energy," in: Proc. 6th Int. Symp., Sept. 2-4, 1981, London.
3. O. Cohen, "Relative risk studies and their relevance to decision-making: the analytical approach in perspective," in: Proc. 6th Int. Symp., Sept. 2-4, 1981, London.
4. V. A. Kirillin, The Development of Power Engineering [in Russian], MTsNTI, Moscow (1981).
5. Electric Power of the USSR in 1981 [in Russian], Informénergo, Moscow (1982).
6. A. A. Makarov and A. G. Vigdorchik, The Fuel—Power Complex [in Russian], Nauka, Moscow (1979).
7. S. Ya. Chernavskii, The Systematic Prediction of Nuclear Power [in Russian], Nauka, Moscow (1980).

OPTIMIZING THE PARAMETERS OF A SHIP-BORNE NUCLEAR POWER PLANT ON A COMBINED CRITERION

V. N. Dolgov

UDC 621.039.578

By parameter optimization for nuclear power plant (NPP) one understands the use of a special mathematical technique to determine the values of the parameters in the technically permissible range providing the optimum values for the parameters taken as criteria, provided that these obey all the constraints on the design and operation.

Parameter optimization for NPP, as for any other complex system, is meaningful if the object is specified. This should be done at the early stages of design, where the necessary input data have been accumulated but it is still possible to use the optimization results in the subsequent stages.

The object in an NPP is characterized by the type of plant, the essential scheme and the assembly scheme, the equipment composition and features, and the operating states of the mechanisms and materials. These parameters may be called constructional and assembly ones, and they largely determine the reliability, construction and operating costs, flexibility, and so on, which in turn govern the performance of the hierarchic system at a higher level. These plant parameters are much less dependent on the optimized parameters within a given type of design than are the dimensions or the thermal economy. Therefore, one can use the mass, dimensions, and thermal economy as criteria in developing research methods and in parameter optimization, or the relative quantities K_G (kg/kW), K_V (m^3/kW), and η_e.

Clearly, the conditions may give rise to various optima, for example, in the mass, dimensions, or thermal economy. Correspondingly, the optimum values of the adjustable parameters differ.

In other words, one set of parameters will provide the minimum mass, another will provide the maximum thermal efficiency, etc. These optima are defined as follows. Experience with designing and building power plants enables one to find the limiting values for the mass criterion K_G^{li}, the dimensions K_V^{li}, and the thermal efficiency η_e that can be attained at present. Then one considers various combinations of the parameters and draws up calculated values of K_G, K_V, and η_e together with the limiting values and rules out those forms that do no satisfy the following conditions:

$$K_G \leqslant K_G^{li}; \quad K_V \leqslant K_V^{li}; \quad \eta_e \geqslant \eta_e^{li}.$$

Out of the forms remaining, one selects those with minimal values for the mass and dimensions and the maximum value for the thermal efficiency.

In practice, it is often necessary to define one such form in which the mass, size, and thermal efficiency are simultaneously as close as possible to the extreme values. We consider the combined curves shown in $K_G - K_V$, $K_V - \eta_e$ and $\eta_e - K_G$ coordinates in Fig. 1, which have been obtained for single-unit high-power NPP.

These curves have been constructed pointwise, with the points obtained as follows. Each parameter combination corresponds to a form of NPP with certain values of K_G, K_V, and η_e, and from these one selects forms having functions $K_G = f_1(K_V)$; $K_V = f_2(\eta_e)$; $\eta_e = f_3(K_G)$, monotonically varying from the extreme values to values corresponding to turning points in the arguments K_V^{min}, η_e^{max} and K_G^{min}. On the graph for $K_G = f(K_V)$, for example, here one shows only those parameter combinations (points) that provide the minimum possible value of K_V with a given value for K_G. The graph shows that improvement in K_G involves deterioration in K_V and η_e, i.e., these different parameters vary in a conflicting fashion in the region of the turning-point values.

Translated from Atomnaya Énergiya, Vol. 57, No. 5, pp. 336-341, November, 1984. Original article submitted September 30, 1983.

 0038-531X/84/5705-0762$08.50

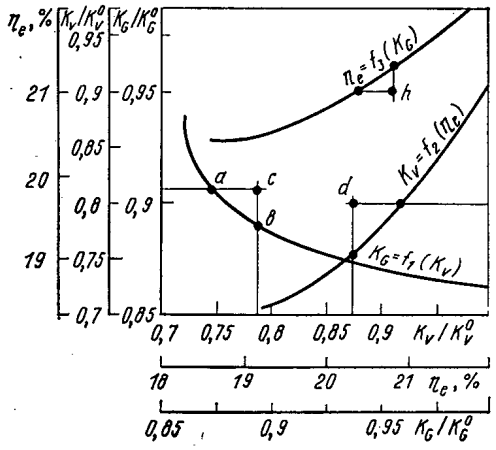

Fig. 1. Optimality curves for power plants.

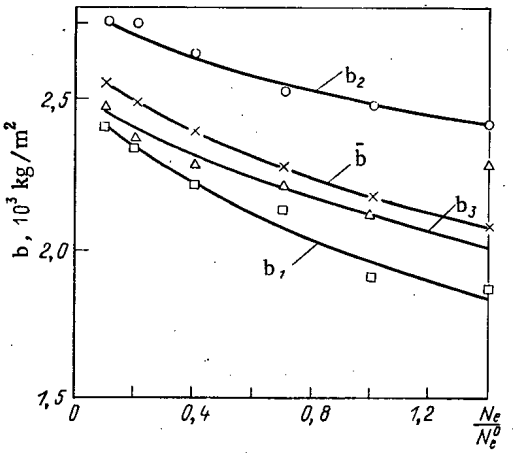

Fig. 2. Dependence of K_G/K_V on effective NPP power ($b = K_G/K_V$): □) for K_G^{min}; Δ) for η_e^{max}; ○) for K_V^{min}; ×) under optimum conditions.

The curves of Fig. 1 have some features of practical significance. Firstly, the points on these curves show how the least (largest) value can be taken by one criterion without increase (decrease) in another. Secondly, the locus of the points characterizes a compromise (optimal) solution on the basis of competing criteria. Thirdly, points away from the optimality curves (for example, c, d, or h) show that the performance criteria for systems corresponding to these points can be improved in at least two ways. In other words, any point or segment such as a-b on the $K_G = f_1(K_V)$ curve corresponds to a plant whose parameters are better than those of a plant characterized by c. Finally, the optimality curves divide up the space into two regions. The region above the $K_G = f(K_V)$ and $K_V = f(\eta_e)$ curves characterizes real or future systems, while the region below the curves characterizes systems that cannot be realized. On the other hand, for the space of $\eta_e = f_3(K_G)$, the region of real systems lies below the curve and the region of unreal ones above it. One can solve a problem with several conflicting criteria by computer. Various methods are used in this country and elsewhere, which involve two different approaches.

The first approach is that the problem with several criteria is reduced to one with one, in which the other criteria are used as constraints. A deficiency of this approach arises from the difficulty in choosing the constraints quantitatively.

The second approach uses a combined criterion, namely a linear combination of the individual criteria with appropriate weighting coefficients. The expression for the combined criterion is [1, 2]

$$F = \varphi_1 f_1(u) + \varphi_2 f_2(u) + \ldots + \varphi_n f_n(u), \qquad (1)$$

where d is the optimized-parameter vector, r_1, r_2, ..., r_n are the partial criteria, and φ_1, φ_2, ..., φ_n are the weighting coefficients. This approach enables one to define the optimum form, but expert evaluations are needed to choose the weighting coefficients.

The expression for the combined criterion for an NPP can be put in the form of (1), where φ_1, φ_2, and φ_3 incorporate the dependence of the mass, dimensions, and thermal efficiency on the requirements of the superior system.

Axiomatic methods are used in solving such problems for complex systems such as ship NPP, which are based on the classical theory of expected utility, and whose essence is presented for example in [2].

Figure 1 implies that the parameters of an NPP are not additive, which means in practice that with a given effective power and given values for any two parameters, the third can take several values, including the limiting permissible one for the given scientific and technical level. Therefore, there exists a form of NPP whose mass, dimensions, and thermal efficiency are simultaneously closest to the extreme ones.

This circumstance provides a basis for developing a method of handling multicriterion optimization for ship NPP without involving expert evaluations. A combined criterion must satisfy the following requirements: improvement in the criterion should not conflict with improvement in the performance of the hierarchic system at a higher level (the ship), while the criterion should be sensitive to the optimized parameters and should be determined from the model for the relevant hierarchic level.

Then the combined criterion can be formulated as

$$K_{opt} = K_G + \bar{b}K_V + c\frac{1}{\eta_e}, \qquad (2)$$

where $\bar{b} = K_G^{min}/K_V^{min}$ and $\bar{c} = K_G^{min}\eta_e^{max}$ are correspondingly the specific mass (in kg/m³) and the mass equivalent to unit thermal power (in kg/kW) as calculated from the extreme values of the partial criteria.

The first term on the right in this equation is the relative power plant mass, while the second and third terms are correspondingly the relative volume and thermal efficiency expressed in terms of the relative mass. In other words, K_{opt} is the reduced relative mass (in kg/kW).

Expression (2) can be put as

$$K_{opt} = \frac{G_{NPP}}{N_e}\left(1 + \frac{G_{NPP}^{min}}{G_{NPP}}\frac{V_{NPP}}{V_{NPP}^{min}} + \frac{G_{NPP}^{min}\eta_e^{max}}{G_{эу}\eta_e}\right).$$

The structure shows that K_{opt} is equal to three times the relative mass if the mass and dimensions are minimal and the thermal efficiency is maximal, i.e., in the ideal case, which does not exist. For real forms, K_{opt} is always more than three times the ratio of the minimal mass to the effective power. The excess of K_{opt} over $3G_{NPP}^{min}/N_e$ is a measure of the deviation from parameter optimality. This means that the best form is that in which K_{opt} is lowest.

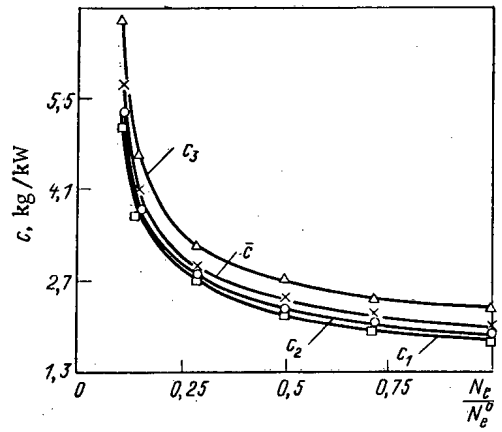

Fig. 3. Dependence of $K_G\eta_e$ on the effective power ($c = K_G\eta_e$): □) for K_G^{min}; Δ) for η_e^{max}; ○) for K_V^{min}; ×) under optimum conditions.

TABLE 1. Calculated Results for K_{opt} in kg/kW

α	β	γ	$\bar{b}\times10^3$, kg/m³	$\bar{c}$, kg/kW	K_{opt} I	II	III	IV	V
1,0	1,0	1,0	2,18	2,16	34,8	31,4	30,6	32,2	30,2
2,0	0,5	0,5	2,05	2,08	33,7	30,8	29,6	31,1	29,2
0,5	2,0	0,5	2,34	2,11	35,2	32,0	31,0	33,7	29,2
0,5	0,5	2,0	2,16	2,30	35,3	32,0	31,1	32,6	30,8
0,1	2,8	0,1	2,47	2,08	34,4	32,5	31,4	33,3	31,1
2,8	0,1	0,1	1,96	2,02	33,0	29,5	28,9	30,4	28,5
1,5	1,0	0,5	2,15	2,09	34,2	31,0	30,2	31,8	29,8
2,5	0,25	0,25	1,99	2,04	33,2	29,9	29,9	30,7	28,8
0,7	0,5	1,8	2,14	2,27	35,0	31,8	31,0	32,4	30,6
0,5	0,7	1,8	2,19	2,27	35,3	32,0	31,1	32,7	30,8
0,1	0,1	2,8	2,10	2,40	35,2	31,8	31,0	32,4	30,6
0,0	0,0	3,0	2,13	2,43	36,0	32,3	31,7	**33,1**	31,2
3,0	0,0	0,0	1,92	2,00	32,6	29,4	28,7	**30,2**	28,2

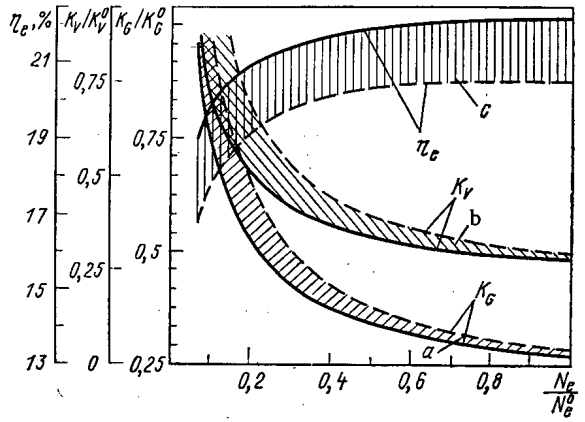

Fig. 4. Nomogram for the variation in performance criteria: solid line – extremal values of criteria; dashed lines - attained values for criteria.

This shows that with a given effective power the coefficients b and c in (2) should be independent of the performance criteria and have physical significance. Figure 2 shows $b_i(N_e)$ curves characterizing the dependence of K_G/K_V on the effective power as found for three optimal forms, in each of which there is an extreme value for one of the criteria, i.e., either minimum mass (form K_G^{min}) or minimum dimensions (form K_V^{min}) or else maximal thermal efficiency (form η_e^{max}).

The corresponding $b_1(N_e)$, $b_2(N_e)$ and $b_3(N_e)$ curves have the physical meaning of the specific mass. The graph also shows the averate relation (in kg/m³)

$$\bar{b}(N_e)=\frac{b_1(N_e)+b_2(N_e)+b_3(N_e)}{3}.$$

Figure 3 shows the dependence of $c_i = K_{Gi}\eta_{ei}$ on the effective power constructed for the same forms as for the curves in Fig. 2. The physical meaning of the Fig. 3 curves is mass per unit thermal power produced by the apparatus.

Table 1 gives calculations on K_{opt} for five different combinations I-V of the optimized parameters. The calculations were performed for a large number of combinations of α, β, and γ, which express correspondingly the dependence on the minimal mass (coefficients b_1 and c_1), the minimum dimensions (b_2 and c_2), and the maximal thermal efficiency (b_3 and c_3).

Table 1 shows that the highest value of K_{opt} corresponds to form I, no matter what the values of α, β, and γ; also, as K_{opt} decreases, one finds forms providing the maximum thermal efficiency (form IV), the minimum mass (form II), and the minimum dimensions (form III).

The lowest K_{opt} occurs for V. Therefore, the optimality of the forms, i.e., their distribution over the decreasing values of K_{opt}, is independent of the significance of the extreme values of the criteria. This occurs because $\bar{b}$ and $\bar{c}$, which correspondingly characterize the specific mass and the mass equivalent to unit thermal power, are independent of the preference for the criteria K_G, K_V, and η_e, as is evident from Figs. 2 and 3.

Form V was defined from calculations with a BÉSM-6 computer on the various forms and on optimizing the parameters on the combined criterion of (2).

Figure 4 illustrates the performance of this method as a nomogram for the variations in the criteria, which shows the levels of the extreme values of K_G, K_V, and η_e (found by optimizing the parameters) as well as those attained in practice. The points a, b, and c denote the values for form V. These points lie in the hatched region, which corresponds to values of the criteria better than those attained in practice, so one concludes that these points belong to the optimum form.

This means that (2) is justified as an expression for K_{opt}, and this implies an important conclusion for use in parameter optimization. One can define the optimum form that provides simultaneously near-extremal values for the mass, dimensions, and efficiency by using one of the methods for locating extreme points such as ordering the form on a performance criterion as given in [3, 4] to find the form in which one of the criteria is equal to the extreme value. Then the data for this form are used to determine the pairs of coefficients b_1 and c_1 (in the case of minimal mass), b_2 and c_2 (minimal dimensions), or b_3 and c_3 (maximum thermal efficiency), which are substituted into (2) instead of $\bar{b}$ and $\bar{c}$. One then examines all the forms to identify the one with the least K_{opt}, which will be the optimum one, since this has the best parameters in mass, dimensions, and thermal economy (points a, b, and c in Fig. 4).

Analogous results are obtained if one uses not the reduced relative mass but the reduced relative volume or reduced thermal efficiency as the combined criterion. Then the expressions for this are

$$K'_{opt} = K_V + \frac{1}{\bar{b}} K_G + \frac{\bar{c}}{\bar{b}} \frac{1}{\eta_e}; \tag{3}$$

$$K''_{opt} = \eta_e + \bar{c} \frac{1}{K_G} + \frac{\bar{c}}{\bar{b}} \frac{1}{K_V}. \tag{4}$$

Here $\bar{b}$ and $\bar{c}$ have the same values as in (2). However, it should be borne in mind when using (4) that the best form is that with the highest K_{opt}.

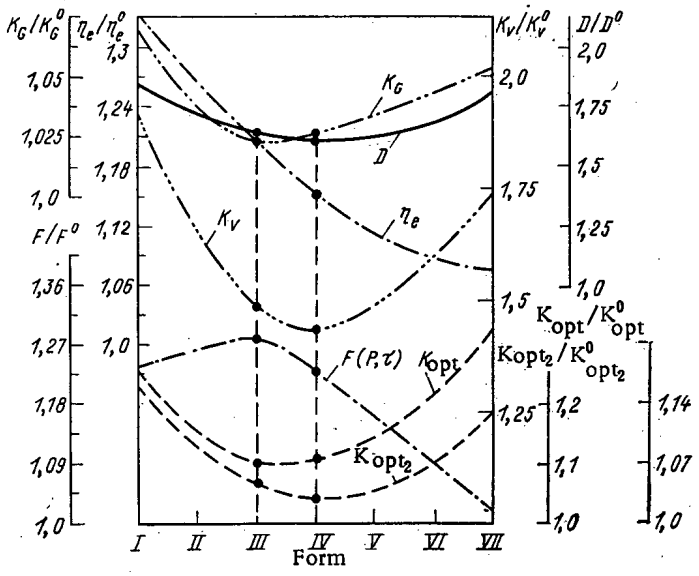

Fig. 5. Effects of mass and dimensions together with the thermal efficiency on the displacement D and load capacity F (here K_{opt} means K_{opt_1}).

Then (2)-(4) enable one to find parameter combinations providing mass and size economy in the NPP for a given load capacity of the ship, which thus reduces the displacement. Also, the optimum forms found by means of combined criteria provide a lower ratio of the reactor thermal power to the volume of the fuel-pin cores because of the higher thermal efficiency. This improves the working life before the fuel pins have to be exchanged with given values for the nonuniformity of the heat production in the pins and the limiting permissible fission-product concentration, and this increases the time τ the ship can spend at sea. At the same time, the optimum form enables one to increase the load capacity P because of the improvement in the mass and dimensions for a given displacement. These two factors determine the load carrying capacity $F(P, \tau)$ under otherwise equal conditions.

If we assume that $F(P, \tau)$ is continuous, monotone, and differentiable in the working region, we have

$$\Delta F = \sum_{i=1}^{n} \frac{\partial F}{\partial y_i} \Delta y_i = \frac{\partial F}{\partial P} \Delta P + \frac{\partial F}{\partial \tau} \Delta \tau = \\ = \frac{\partial F}{\partial P} \left(\frac{\partial P}{\partial K_G} \Delta K_G + \frac{\partial P}{\partial K_V} \Delta K_V \right) + \frac{\partial F \partial \tau}{\partial \tau \partial \eta_e} \Delta \eta_e, \tag{5}$$

where $\partial F/\partial y_i$ is the increment in the load capacity due to change in parameter i, Δy_i is the change in parameter i of the ship due to change in plant parameters, and $\partial F/\partial K_G$, $\partial P/\partial K_V$, $\partial \tau/\partial \eta_e$ are the increments in the load capacity and time at sea due to changes in the mass and dimensional parameters and the thermal efficiency, while ΔK_G, ΔK_V, $\Delta \eta_e$ are the changes in the mass and dimensional parameters and thermal economy produced by altering plant parameters.

We see from (5) that the load capacity is dependent on the mass and dimensions of the NPP as well as the thermal efficiency. Figure 5 shows the variation in this function with combinations of the parameters for a hypothetical ship. The maximum $F(P, \tau)$ corresponds to minimum K_{opt_1}, which indicates that this quantity is a quantitative measure of the load capacity and is amongst the major parameters determining the economic performance.

The combined criterion can be used also to determine parameter combinations providing the minimum displacement. In that case, the last term should be eliminated from (2), which incorporates the effect of the thermal efficiency on the displacement. Then in kg/kW the expression for the combined criterion is

$$K_{opt_2} = K_G + \bar{b} K_V. \tag{6}$$

Figure 5 shows the dependence of K_{opt_2} on the parameter combinations and the corresponding displacement D.

This method of combining the parameters enables one to handle optimizations with four or more competing criteria, e.g., when one incorporates the cost of constructing the power plant. In that case, the expression for the combined criterion contains a further term with appropriate coefficient. The method is also applicable not only to nuclear power plant but also to plant of any other type.

The following conclusions are drawn:

1) A method has been proposed for optimizing power-plant parameters in the case of three competing indices: mass, dimensions, and thermal efficiency;

2) expressions (2)-(5) may be used as combined criteria for evaluating the performance, these being combinations of K_G, K_V, and η_e with the coefficients $b = \frac{K_G}{K_V}$ and $c = K_G \eta_e$, determined from the extremal values of the individual performance criteria;

3) the combined criterion is a quantitative measure of the ship load capacity and belongs to the major factors determining the economic efficiency (expression (2)).

LITERATURE CITED

1. Engineering Design and Technology: Proceedings of the American Society of Mechanical Engineers [Russian translation], No. 1, Mir, Moscow (1974).
2. R. L. Keeny and H. Raifa, Decisions with Multiple Criteria: Preferences and Substitution [Russian translation], Radio i Svyaz', Moscow (1981).

3. V. N. Dolgov, Parameter Optimization of Ship Nuclear Power Plants [in Russian], Sudostroenie, Leningrad (1980).
4. A. S. Popyrin, Simulation and Optimization for Thermal Power Plants [in Russian], Énergiya, Moscow (1978).

CONTINUOUS MARKOV PROCESSES IN WORKING-LIFE ESTIMATION WITH REFERENCE TO AN RBMK-1000 CONTROL VALVE

A. I. Klemin, V. S. Emel'yanov, and A. V. Rabchun

UDC 621.08.004:6:621.039

A current problem in reliability analysis for nuclear power plant (NPP) is to provide scientific evaluation of the working-life parameters at the design and operating stages. A possible method is based on examining the random aging processes occurring in the items, which lead to viability failure as a whole. The aging is characterized by irreversible changes in the state due to external and internal factors, and this can be described by a function called the aging parameter (AP) [1]. The AP for a component may be taken for example as the parameter in the flux of failures, the mean down time for repair during a given working period, or else, as for the pressure control valve PCV in the RBMK-1000, the torque required to open or close the valve.

When the random process describing the AP reaches a certain value, one can consider that the item has reached a limiting state. Therefore, the statistical characteristics of the instant when the process attains a given limit may be taken as the working-life characteristics. Some tasks in estimating working life, including for NPP equipment, may be formulated mathematically as estimating the characteristics for the first attainment of a given boundary or limit by the random process describing the AP.

Three types of boundary are distinguished in the theory of random processes: transparent, absorbing, and reflecting.

In practical reliability estimation, the possible range for the ordinate is usually bounded by two screens, since these problems relate to determining the bounds to a random process (we consider only one-dimensional random processes). Here the following situations are possible: the physical essence of the AP is such that it cannot be less than a certain value (for example, zero), while the AP exceeding a specified value leads to failure in the item; or if the AP exceeds any of the bounds, the item fails. In the first case, one bound is to be considered as reflecting and the other as absorbing. In the second case, both bounds are absorbing.

The attainment of given bounds by a random process has a regular solution for a Markov diffusion process, which can be used to describe actual aging processes, as is shown below [2, 3]. The basic statistical characteristic is the conditional transition probability $\pi(x, t|x_0, t_0)$, which is the probability density that the process is in state x_0 at time t_0 and is in state x at time t. We know that $\pi(x, t|x_0, t_0)$ obeys the direct and inverse Kolmogorov equations, which take the following form for a one-dimensional continuous Markov diffusion process [2]:

$$\frac{\partial}{\partial t}\pi(x, t \mid x_0, t_0) = -\frac{\partial}{\partial x}[A(x, t)\pi(x, t \mid x_0, t_0)] + \frac{1}{2}\frac{\partial^2}{\partial x^2}[B(x, t)\pi(x, t \mid x_0 t_0)]; \quad (1)$$

$$-\frac{\partial}{\partial t_0}\pi(x, t \mid x_0, t_0) = A(x_0, t_0)\frac{\partial}{\partial x_0}\pi(x, t \mid x_0, t_0) + \frac{1}{2}B(x_0, t_0)\frac{\partial^2}{\partial x_0^2}\pi(x, t \mid x_0, t_0), \quad (2)$$

where A(x, t) is of the nature of a transport coefficient, which is equal to the limit to the ratio of the mathematical expectation for the difference in the ordinates to the time interval for which these ordinates are considered when the interval tends to zero, while B(x, t) is the diffusion coefficient, which is equal to the limit of the ratio of the mathematical

Translated from Atomnaya Énergiya, Vol. 57, No. 5, pp. 341-346, November, 1984. Original article submitted August 25, 1983.

 0038-531X/84/5705-0768$08.50

expectation for the square of the difference in the ordinates to the time interval as the latter tends to zero. The definitions of these coefficients are

$$A(x, t) = \lim_{\Delta t \to 0} \left(\frac{1}{\Delta t}\right) \int [x(t + \Delta t) - x(t)]\, \pi(x, t + \Delta t \mid x, t)\, dx;$$

$$B(x, t) = \lim_{\Delta t \to 0} \left(\frac{1}{\Delta t}\right) \int [x(t + \Delta t) - x(t)]^2\, \pi(x, t + \Delta t \mid x, t)\, dx.$$

In considering the attainment of set bounds by a continuous Markov diffusion process, it is convenient to replace $\pi(x, t|x_0, t_0)$ by the transition probability density for paths that never reach the bounds $p(x, t|x_0, t_0)$. It has been shown [4] that $p(x, t|x_0, t_0)$ also obeys (1) and (2).

If we know $p(x, t|x_0, t_0)$, we can determine the probability $p_{c,d}(x_0, t)$ that the continuous process attains given bounds at the points x = c and x = d as follows:

$$p_{c,d}(x_0, t) = 1 - \int_c^d p(x, t \mid x_0, t_0)\, dx. \tag{3}$$

Equations (1) and (2) are of parabolic type. Initial and boundary conditions must be supplied in order to derive $p(x, t|x_0, t_0)$ as solutions to (1) or (2). If the start of the process is specified, the following condition may be used as the initial one:

$$p(x, t \mid x_0, t_0)\,|_{t=t_0} = \delta(x - x_0).$$

If the ordinates X(t) at the initial instant are distributed with probability density $p_0(x)$, the initial condition is written as

$$p(x, t \mid x_0, t_0)\,|_{t=t_0} = p_0(x).$$

The boundary conditions are determined by the type of boundary. If the boundary at d is absorbing, the boundary condition is

$$p(d, t \mid x_0, t_0) = 0,$$

and if it is reflecting

$$\frac{\partial}{\partial x_0} p(x, t \mid x_0, t_0)\,|_{x_0 = d} = 0.$$

In the case of an absorbing screen, the normalization condition for $p(x, t|x_0, t_0)$ is not obeyed, since with the passage of time an increasing number of the paths will attain the boundary and will be lost to further consideration, i.e., $\int_{-\infty}^{d} p(x, t \mid x_0, t_0)\, dx < 1$. A feature of the reflecting screen is that the number of paths is constant at any instant, i.e., the condition of normalization to one should be obeyed:

$$\int_{-\infty}^{d} p(x, t \mid x_0, t_0)\, dx = 1.$$

In the case of two screens at c (reflecting) and d (absorbing), we may note the following feature, which sometimes enables one to simplify deriving some characteristics:

$$\int_{-\infty}^{d} p^*(x, t \mid x_0, t_0)\, dx = \int_c^d p(x, t \mid x_0, t_0)\, dx, \tag{4}$$

where $p^*(x, t|x_0, t_0)$ is the transition probability density found by solving the Kolmogorov equation as x varies from $-\infty$ to d and $p(x, t|x_0, t_0)$ is the same for the boundary-value problem $(c \leqslant x \leqslant d)$.

The time T_γ for the first attainment of the boundaries with a given probability γ can be calculated if we know $p_{c,d}(x_0, t)$ and solve the equation

$$1 - p_{c,d}(x_0, T_\gamma) = \gamma.$$

With the above assumptions, T_γ may be considered as the γ percent working life of the item. To estimate this parameter, which is determined by the integral of $p(x, t|x_0, t_0)$, in cases of reflecting and absorbing screens, we use (4) and find the integral of $p(x, t|x_0, t_0)$ for a semiinfinite range in the coordinate. If both boundaries are absorbing, the only approach is to solve (1) with zero boundary conditions.

Therefore, if the wear in NPP equipment is characterized by an ageing parameter, and the variation in this is described by a continuous Markov process X(t), the working-life parameters may be determined from the known probability density $p(x, t|x_0, t_0)$ for X(t), which is found from (1) or (2) with the corresponding initial and boundary conditions. To solve this problem, it is necessary to determine the transport and diffusion coefficients.

As NPP equipment is expensive, tests can give only a small number of realizations for the AP for it. In that case, it is impossible to estimate A(x, t) and B(x, t) statistically as functions of x and t, i.e., one cannot estimate the effects of the coordinate on these coefficients, and one can only obtain estimators either as time dependencies A(t) and B(t) or consider the case of coefficients A and B constant in time.

One can obtain point and integral estimators for these coefficients from a restricted number of realizations. We assume that tests of duration from t_0 to T have given N_p realizations of the one-dimensional random process X(t) describing the AP for some item.

Dub's theorem [5] implies that a one-dimensional continuous process is a Markov one if the random increments in the process during small nonoverlapping time intervals Δt are statistically independent, while the ordinate has a normal distribution. To find Δt, we proceed as follows. In the interval $[t_0, T]$ we select two nonoverlapping intervals of arbitrary length $\Delta\tau$. We estimate the autocorrelation function for the increments in X(t) for these two nonoverlapping intervals of length $\Delta\tau$ by reference to N_p realizations:

$$\hat{K}(\Delta\tau, \Delta\tau) = \frac{1}{N_p - 1} \sum_{j=1}^{N_p} \left\{ \left[\Delta x_j^{(1)} - \frac{1}{N_p} \sum_{j=1}^{N_p} \Delta x_j^{(1)} \right] \left[\Delta x_j^{(2)} - \frac{1}{N_p} \sum_{j=1}^{N_p} \Delta x_j^{(2)} \right] \right\}, \tag{5}$$

where $\Delta x_j^{(1)}$ and $\Delta x_j^{(2)}$ are the random increments in X(t) correspondingly in the first and second intervals of length $\Delta\tau$ each for realization j. We vary $\Delta\tau$ to find a value $\Delta\tau = \Delta$ such that the autocorrelation of (5) is equal to zero or sufficiently close to it. If the conditions of Dub's theorem are obeyed, X(t) may be considered approximately as a Markov process for intervals $\Delta t > \Delta$.

To estimate the transport and diffusion coefficients for X(t), we split up the interval $[t_0, T]$ into intervals Δt ($t_0 < t_1 < \ldots t_i \ldots < t_{n-1} < t_{nt} = T$), whose duration is determined from the condition for statistical independence in the increments.

The definitions of the coefficients mean that point estimators for these can be obtained at each instant t_i as follows:

$$\hat{A}(t_i) = \frac{\hat{m}_x(t_i) - \hat{m}_x(t_i - \Delta t)}{\Delta t} = \frac{\sum_{j=1}^{N_p} [x_j(t_i) - x_i(t_i - \Delta t)]}{N_p \Delta t}; \tag{6}$$

$$\hat{B}(t_i) = \frac{\hat{D}_x(t_i) - \hat{D}_x(t_i - \Delta t)}{\Delta t} = \frac{\sum_{j=1}^{N_p} \{[x_j(t_i) - \hat{m}_x(t_i)]^2 - [x_j(t_i - \Delta t) - m_x(t_i - \Delta t)]^2\}}{(N_p - 1)\Delta t}, \tag{7}$$

where $\hat{m}_X(t_i)$ is the estimator for the mathematical expectation of X(t) at time t_i, $\hat{D}_X(t_i)$ is the estimator for a variance of X(t) at t_i, and $x_j(t_i)$ is the ordinate of X(t) at t_i obtained for realization j.

The error in these point estimators is determined by N_p. The accuracy of the estimators given by (6) and (7) can be determined by using the concepts of confidence range and confidence probability. The errors in the estimators are determined by those in the mathematical expectation and variance for $X(t_i)$ at the instants t_i.

It follows from Dub's theorem [5] that the coordinate of a Markov diffusion process has a normal distribution at any instant. In that case, the lower and upper confidence limits to the true values of the mathematical expectation and variance at time t_i are given by the following:

$$m_x^l(t_i) = \hat{m}_x(t_i) - t_\beta \sqrt{\frac{\hat{D}_x(t_i)}{N_p}};$$

$$m_x^u(t_i) = \hat{m}_x(t_i) + t_\beta \sqrt{\frac{\hat{D}_x(t_i)}{N_p}};$$

$$\hat{D}_x^l(t_i) = \frac{\hat{D}_x(t_i)}{\chi_1^2}(N_p - 1); \quad D_x^u(t_i) = \frac{\hat{D}_x(t_i)}{\chi_2^2}(N_p - 1),$$

where t_β is the quantile of the Student's t distribution, while χ_1^2 and χ_2^2 are the quantiles of the χ^2 distribution defined from the given values of the probability β and the value of N_p, the number of realizations of the random process X_p. The confidence limits to the true values of the coefficients at these instants t_i are given by

$$A^l(t_i) = \frac{m_x^l(t_i) - m_x^l(t_i - \Delta t)}{\Delta t}; \tag{8}$$

$$A^u(t_i) = \frac{m_x^u(t_i) - m_x^u(t_i - \Delta t)}{\Delta t};$$

$$B^l(t_i) = \frac{D_x^l(t_i) - D_x^l(t_i - \Delta t)}{\Delta t}; \tag{9}$$

$$B^u(t_i) = \frac{D_x^u(t_i) - D_x^u(t_i - \Delta t)}{\Delta t}.$$

In a particular case, one can take the coefficients as constant, i.e., $\hat{A}(t_i) = \text{const} = \hat{A}$ and $\hat{B}(t_i) = \text{const} = \hat{B}$; then the procedure for estimating the time of first attainment of given bounds by X(t) amounts to solving (1) or (2) either with coefficients A(t) and B(t), in which case Kolmogorov's equation can be solved by numerical methods, e.g., the pivot method [6], or with constant values A and B (in the latter case, an analytic solution exists).

We consider the case of attaining a single absorbing boundary at x = d by reference to a continuous one-dimensional Markov diffusion process with constant transport and diffusion coefficients. The boundary-value problem for the probability density $p(x, t | x_0, t_0)$ takes the form

$$\frac{\partial}{\partial t} p(x, t \mid x_0, t_0) = -A \frac{\partial}{\partial x} p(x, t \mid x_0, t_0) + \frac{B}{2} \frac{\partial^2}{\partial x^2} p(x, t \mid x_0, t_0); \tag{10}$$

$$p(x, 0, x_0) = \delta(x - x_0);$$

$$p(-\infty, t, x_0) = 0;$$

$$p(d, t, x_0) = 0.$$

The solution is

$$p(x, t, x_0) = \frac{1}{\sqrt{2\pi B t}} \left\{ \exp\left[-\frac{(x - x_0 - At)^2}{2Bt} \right] - \exp\left[-\frac{(x + x_0 - 2d - At)^2 - 4At(d - x_0)}{2Bt} \right] \right\}.$$

As the final task is to determine the probability or time of attaining the boundary, we calculate the integral distribution:

$$p(x, t) = \Phi\left(\frac{x - x_0 - At}{\sqrt{Bt}} \right) - \exp\left[\frac{2A(d - x_0)}{B} \right] \Phi\left(\frac{x + x_0 - 2d - At}{\sqrt{Bt}} \right),$$

where

$$\Phi(z) = \frac{1}{\sqrt{2\pi}} \int_{-\infty}^{z} \exp\left(-\frac{x^2}{2}\right) dx.$$

Then the probability of attaining the bounds is

$$p_d(x_0, t) = 1 - P(d, t) = 1 - \Phi\left(\frac{d - x_0 - At}{\sqrt{Bt}}\right) + \exp\left[-\frac{2A(d-x_0)}{B}\right]\Phi\left(\frac{x_0 - d - At}{\sqrt{Bt}}\right). \quad (11)$$

In (11), the difference of the term containing the exponential from zero shows how far the solution for a semiinfinite range in the coordinate differs from that for an infinite range. The value of this term is determined mainly by the value of the exponential.

The value of T_γ can be determined for a known integral distribution for P(d, t) by solving

$$\gamma = 1 - P(d, T_\gamma) = \left[\Phi\left(\frac{d - x_0 - AT_\gamma}{\sqrt{BT_\gamma}}\right) - \exp\left[-\frac{2A(d-x_0)}{B}\right]\Phi\left(\frac{x_0 - d_0 - AT_\gamma}{\sqrt{BT_\gamma}}\right)\right]. \quad (12)$$

The following equation gives the mathematical expectation $M[T] = T_0$ for the time for first attainment of the absorbing boundary $x = d$ for a continuous one-dimensional Markov diffusion process with constant coefficients:

$$\frac{B}{2}\frac{d^2T_0}{dx_0^2} + A\frac{dT_0}{dx_0} = -\varphi(x_0) \quad (13)$$

with the boundary conditions

$$T_0(d) = 0 \quad \text{(absorbing screen);}$$
$$\left.\frac{dT_0}{dx_0}\right|_{x_0=c} = 0 \quad \text{(reflecting screen).}$$

Equation (13) follows directly from Pontryagin's equation [4]. The function $\varphi(x_0)$ is the probability of first attainment of one of the boundaries, for example d. In particular, when there are two screens (absorbing and reflecting)

$$\varphi(x_0) = \frac{1 - \exp(-2Ax_0/B)}{1 - \exp(-2Ad/B)}.$$

The following formula defines the mathematical expectation for the time of first attainment of absorbing boundary d if the reflecting boundary is not reached:

$$T_d(x_0) = \frac{d - x_0}{[1 - \exp(-2Ad/B)]} + \frac{B}{2}\frac{1 - \exp(-2Ad/B)}{1 - \exp(-2Ax_0/B)} - \quad (14)$$
$$- \frac{B}{A^2} - \frac{1}{[1 - \exp(-2Ad/B)]A}[x_0 \exp(-2Ax_0/B) - d\exp(-2Ad/B)].$$

One can examine the accuracy in the statistical determination of the coefficients with various numbers of realizations by computer simulation of a Markov diffusion process with given probabilities, for example by Monte Carlo methods [7]. One can simulate a one-dimensional process of the above type on the basis that the ordinate at any time has a normal distribution with parameters $(x_0 + At, \sqrt{Bt})$. In that case, the procedure amounts to simulating a normally distributed random quantity with given parameters and fixed times t_i. Simulation showed that the coefficients can be estimated from (6) and (7). For example, from 100 realizations of a process with given transport and diffusion coefficients of 0.35 and 0.72 correspondingly, the point estimators given by these formulas were respectively 0.349 and 0.717.

Simulation also enables one to estimate the relative errors in calculating the coefficients from a restricted number of realizations. Numerical experiments showed that the relative error $\hat{\delta}_A$ in determining the transport coefficient is dependent not only on N_p but also on the coefficients specified in the simulation, while the relative error in determining the diffusion coefficient is dependent only on the number of realizations, and is invariant with respect to A and B. It can readily be shown that $Q = \hat{\delta}_A A/\sqrt{B}$ will be determined only by the number of realizations, as will the relative error in estimating the diffusion coefficient. The statistical study gave $\hat{\delta}_B$ and Q as a function of the number of realizations for a process

TABLE 1. Working-Life Parameters for the Pressure Control Valve in an RBKM-1000

Estimator		Transport coeff., mm/h	Diffusion coeff., mm^2/h	Mean life, number of cycles	97% life, number of cycles
Point		1,81	45,87	264	127
Interval (β=0,95)	Lower bound	0,244	16,24	50	24
	Upper bound	3,39	385,33	1096	623

with constant coefficients. For example, Q = 0.18 and $\hat{\delta}_B$ = 0.25 for $N_p = 10$. Knowing $\hat{\delta}_B$ and Q, one can correct the estimators $\hat{A}$ and $\hat{B}$ for the coefficients.

An engineering analysis of the designs and modes of operation together with operating experience with PCV showed that the working life of the PCV is characterized by that of four components: the bellows unit, the power unit consisting of the threaded lead screw-sleeve pair, and two bearings; also, effects come from the guide surfaces in the body and spindle and from components in the flow part of the valve. A study of the possible PCV failures showed that ones in the lead screw-sleeve pair, the guide surfaces, and the bellows unit directly determine the working characteristics. The extent of damage to these components can be judged from the change in the opening-closing torque. A torque increasing to the limiting value ($\sim$ 196 N·m, which corresponds to 89 mm on the scale of the recording instrument) can be considered as PCV failure, in respect of which the valve is a nonrecoverable item, while the time taken to reach this limiting state is the working life. Also, the random process representing the torque may be represented as a continuous Markov diffusion process. The transport and diffusion coefficients for this were estimated from (6) and (7) to give point estimators and from (8) and (9) to give interval estimators from five realizations. Solution of the boundary-value problems of (10) and (13) gave point and interval estimators for the mean life from (14) and the γ percent life from (12) (see Table 1).

The lower bound to the average life T_{av}^{γ} = 50 cycles may evidently be taken as a pessimistic estimator for the working life. If one assumes that there are 100 complete cycles in 30 years of operation, then these estimators show that further operation for at least 15 years is possible.

LITERATURE CITED

1. A. I. Klemin, V. S. Emel'yanov, and V. S. Moroozv, Calculated Nuclear Power Plant Reliability: the Markov Model [in Russian], Énergoizdat, Moscow (1982).
2. A. V. Matveev, "Estimating the probability of parameteric failure," Izv. Akad. Nauk SSSR, Tekh. Kibern., No. 4, 106-112 (1978).
3. M. G. Kostra, B. V. Pranik, V. G. Sklyar, and V. P. Strel'nikov, "A mathematical model for the working-life exhaustion in low-current electrical contacts on prolonged storage," Nad. Kont. Kach., No. 5, 26-32 (1983).
4. V. I. Tikhonov and M. A. Mironov, Markov Processes [in Russian], Sov. Radio, Moscow (1977).
5. J. Dub, Probability Percentages [Russian translation], IL, Moscow (1956).
6. R. D. Richtmyer and K. W. Morton, Difference Methods for Initial-Valve Problems, Wiley (1967)
7. V. G. Sragovich, "Simulating some classes of random process," Zh. Vychisl. Mat. Mat. Fiz., No. 3, 587-593 (1963).

APPARATUS FOR AUTORADIOGRAPHIC MONITORING OF THE DISTRIBUTION OF PLUTONIUM IN MIXED OXIDE FUEL

I. A. Golenishchev, I. G. Isaev, V. N. Lyubakov, A. N. Maiorov, and V. V. Yampol'skii

UDC 658.56:62.039.154

The uniformity of distribution of plutonium is considered as one of the principal characteristics of mixed oxide fuel, in view of which the appropriate equipment should be provided in the technological line for monitoring the distribution of PuO_2 [1, 2]. The methods and means used at present for monitoring allow both a qualitative [3] and quantitative [4-6] estimate of the PuO_2 distribution to be obtained. Here, the method of α-autoradiography in conjunction with the automatic analysis of the images, providing an objective quantitative estimate of the PuO_2 distribution, opens up broad prospects. However, for this it is necessary to assess quantitatively the accuracy of the reproducibility of this distribution on the autoradiogram, and also to guarantee a constant contrast and resolution.

As the basis for the development of an apparatus, a functional scheme is proposed (Fig. 1) incorporating together with the operations which are universal for α-radiography [7] additionally: increase of contrast of the α-autoradiogram image and setting of the level of discrimination. The introduction of these operations will increase the accuracy of the determination of the sizes of the regions with an enhanced PuO_2 content.

In order to improve the resolution of the image on the α-autoradiograms, the well-known method of installing a collimating filter between the product being monitored and the detector is used [8]. In this case, in place of metal foils it is advantageous to use a double-layer collimator of polyethyleneterephthalate film and an emulsion layer of movie film de-

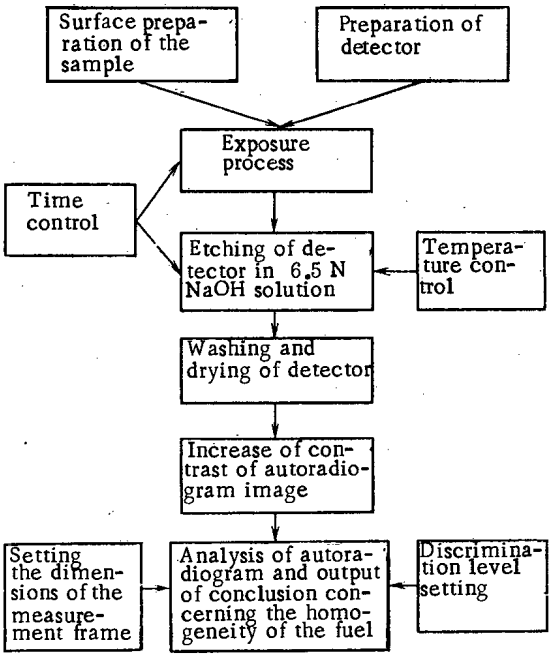

Fig. 1. Functional scheme for monitoring the uniformity of distribution of PuO_2 in mixed oxide fuel, by the method of α-autoradiography.

Translated from Atomnaya Énergiya, Vol. 57, No. 5, pp. 346-349, November, 1984. Original article submitted November 24, 1983.

 0038-531X/84/5705-0774$08.50

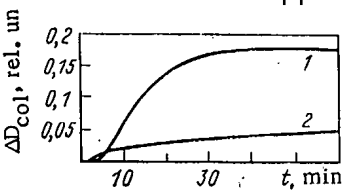

Fig. 2. Variation of contrast of the optical density of the image (1) and background (2) with increase of the duration of coloration of the detectors in a solution of rhodamine in 80% ethyl alcohol.

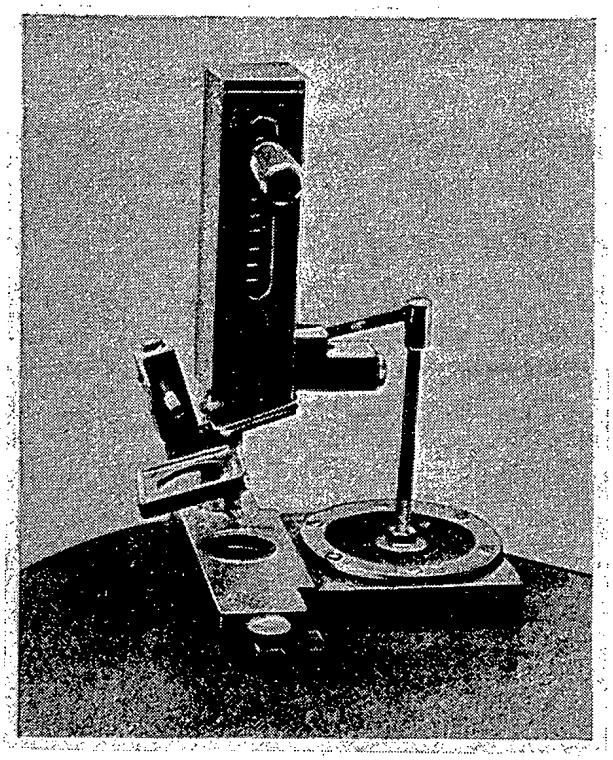

Fig. 3. General view of the device for exposure of the detectors.

posited on the α-radiation detector of nitrocellulose. This will allow the contrast of the image in the dielectric track detector to be increased [9] due to the deposition of the additional layer, which reduces the action of the alkali solution on the unirradiated parts of the detector and increases the reproducibility of the optical density of the image, in consequence of the stabilization of the form of the etched track [10]. The thickness of the layer is chosen in accordance with the requirement for ensuring unambiguity of interpretation of the α-autoradiogram image [11]. In order to increase the contrast of the image, coloration of the developed autoradiogram in a solution of rhodamine in ethyl alcohol is also used.

The maximum increase of the optical density of the image in relation to the optical density of the background is achieved by the use of a saturated solution of rhodamine in 80% ethyl alcohol. Coloring during 30 min (Fig. 2) increases the absolute contrast of the image by 15-25%.

If we take into account that the linear section of the densitometric characteristic curve for the uncolored detector corresponds to an almost tenfold change of the α-particle flux, then as a result of increasing the contrast the necessary number of levels can be discriminated on the autoradiogram, which will ensure distinct perception of the images of regions in which the content of PuO_2 differs by 10 abs.% or more.

In order to carry out the functional scheme for monitoring the uniformity of the PuO_2 distribution in mixed oxide fuel by the method of α-autoradiography, an assembly of equipment has been developed which includes a device for grinding and polishing the pellets, for exposure, for etching the detectors, and also an image television analyzer [11].

The triple-disk facility for grinding and polishing the pellets, similar to that used in metallography, allows the following operations to be carried out successively: roughing on a cast iron disk with grinding powder of electrocorundum with a particle size of more than 40 μm, grinding on a quartz-glass disk with grinding powder with a particle size of ∿ 10 μm,

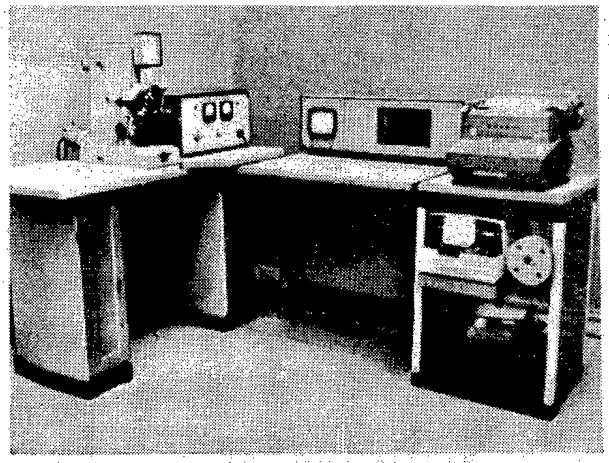

Fig. 4. General view of the television analyzer.

and final polishing on a disk covered with cloth with chromic oxide. For this, a yoke with the pellets, secured in the recess of an actuating lever, performs oscillatory movements over the surface of the disk with a frequency of 13 Hz and rotates around the natural axis under the action of the difference in the peripheral velocities. The design of the actuating lever allows clogging-up of the edges of the yoke and the pellets during grinding to be avoided. The kinematic scheme of the facility provides separate switching of the disks and a smooth change of the frequency of rotation from 17.5 to 750 min^{-1}.

The exposure device (Fig. 3) ensures that a tight and uniform contact is made between the pellets and the detector during a time not exceeding 0.2 sec, which eliminates fuzziness of the image, caused by the movement of the yoke to the detector. The timer allows the duration of exposure to be set in the range from 2 sec to 1 h with an error of not more than 2%.

The television analyzer (Fig. 4) includes a scanning facility, the operator's console and computer equipment. The microscope for operation in transmitted light projects an image, magnified by 15-25 times, of the part of the autoradiogram on the target of the television camera, converting the light flux distribution into a succession of electrical signals which are fed to the videosignal preliminary processing unit. In this unit, digital coding of the video signal is performed according to the pulse amplitude with integral numbers from 0 to 255 and provides an input of discrete information about the optical density distribution to the computer. It should be noted that $\approx$ 200 readings of the analog–digital converter correspond to the dynamic range of the optical density of the autoradiogram image, and regions differing in optical density by 0.05-0.07 relative units are received individually. The quantitative calculation of such parameters of the image as the relative fraction of the area occupied by details of the image with the set interval of optical density, the maximum chord of the image detail, and diameter of the equivalent circle is performed on the computer. The range of discrimination of the optical density signal J(x, y) with respect to each coordinate varies from 2.5 to 5 μm depending on the selected magnification.

The algorithm developed for determining the maximum chord does not require the input of the total image data, but allows data for alternate input of columns of the image to be obtained (Fig. 5). For this, the blocks of coordinates at the beginning and end of transversals, belonging to separate regions and located in a given column, are determined and information about the optical density distribution within the bounds of a column is erased in proportion to the input of the next column and verification of the individual transversals by means of the overlap criterion. As a result, for each individual region, blocks of numbers of $(n - p + 1)$ groups of the form

$$x_{1p}x_{2p} \mid x_{1(p+1)}x_{2(p+1)} \mid x_{1(p+2)}x_{2(p+2)} \mid \ldots \mid x_{1n}x_{2n} \mid,$$

where p and n are the number of the first and last column in which were encountered transversals belonging to the individual region, are stored in the memory.

Then the maximum chord is found (the maximum length of the transversal, joining two points of the outer counter, encompassing the region) as the maximum of the sequence

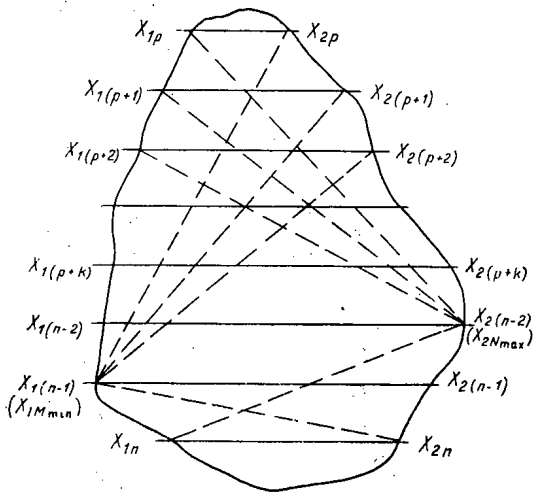

Fig. 5. Example of the determination of the maximum chord of the individual image detail of the autoradiogram.

$$\{\delta_k\} = K\sqrt{(x_{2[(k-1)+p]} - x_{1[n-(k-1)]})^2 + \{[n-(k-1)] - [p+(k-1)]\}^2},$$

where K is a coefficient taking account of the discrimination interval; and k varies from 1 to n − p +1. In order to eliminate the errors which may be introduced by the horseshoe shape of the regions, X_{1m} is chosen minimum and X_{2N} maximum, and the sequences of the distances from the point with coordinates X_{1m} to the point $X_{2\gamma}$ (γ varies from p to n) and from the point X_{2N} to the point $X_{1\gamma}$ are determined and the maximum chord is selected from the three sequences obtained as a result. Simultaneously with the maximum chord, the area of the individual region and the diameter of the equivalent circle and, in proportion to the input of the columns, the running value of the area of the frame being analyzed are computed which, just like the area of the individual region, is equal to the product of the number of points of the television image and the distance between them along the horizontal and vertical.

The conditions used for obtaining the autoradiograms, ensuring a linear relation between the optical density and the enrichment of the region of the PuO_2 pellet in the range from 10 to 100 absolute %, and also the linearity of the light-signal characteristic curve of the videcon in the chosen range of illumination, enable the light flux to be established so that the amplitude of the video signal A_{100}, corresponding to 100% content of PuO_2, occurs on the lower boundary of the linear part of the light-signal characteristic curve. In this case, the discrimination level ensuring the separation on the image of regions containing more than C% of PuO_2 is determined on the basis of the equation

$$A_C = (A_{100} + \alpha)\, 10^{-\frac{0.94}{100}C + 0.94} - \alpha,$$

where A_C is the required level of discrimination, relative units; A_{100} is the amplitude of the video signal, corresponding to 100% content of PuO_2, and α is a constant, the value of which was determined experimentally and is equal to 19 relative units. Having calculated the discrimination level, the geometrical parameters of the image details can be determined, corresponding to regions of the pellet with a PuO_2 content of interest.

The error in measuring the characteristics of the tablet by means of the autoradiogram image analyzer is determined by a number of interrelated factors: fluctuations of the optical density of the autoradiogram image, due to the discrete nature of formation of the image; fluctuations of the amplitude of the television signal; the accuracy of choice of the discrimination level, and also the isotopic composition of the nuclear fuel. Therefore, a quantitative calculation of the error is very difficult.

As a result of the metrological certification report on the equipment assembly it was established that the error in determining the relative fraction of the area occupied by regions with a defined range of content of PuO_2 does not esceed ± 2 absolute %, and the error in determining the geometrical dimensions of the regions of the pellet is not more than ±15 μm.

The analysis of a single pellet by means of the equipment described lasts for not more than 4 h, the preparation of the surface of the pellet occupies from 40 min to 1 h, the process for obtaining the autoradiogram lasts from 10 to 20 min, and the duration of scanning of the autoradiogram does not exceed 2 h.

LITERATURE CITED

1. A. N. Vol'skii and Ya. M. Sterlin, Metallurgy of Plutonium [in Russian], Nauka, Moscow (1967).
2. M. Freshley et al., Nucl. Technol., 15, No. 2, 239 (1972).
3. E. Aitken and S. Evant, Trans. Am. Nucl. Soc., 13, No. 2, 602 (1970).
4. D. Stranik, H. Powers, and G. Last, Trans. Am. Nucl. Soc., 13, No. 2, 603 (1970).
5. J. Butler and D. Clark, J. Nucl. Mater., 33, 208 (1969).
6. J. Spanner and C. Jackson, Mater. Eval., 36, No. 11, 219 (1976).
7. W. Gruber, "Autoradiography of irradiated nuclear ceramic fuels," in: Proceedings of the Seventeenth Conference on Remote Systems Technology (1969).
8. A. Gebers, Nucl. Appl., 5, No. 2, 91 (1968).
9. V. V. Yampol'skii et al., Inventor's Certificate No. 7434.31, Byull. Izobret., No. 12, 291 (1982).
10. D. Peterson, Rev. Sci. Instrum., 41, No. 8, 1252 (1970).
11. I. A. Golenishchev et al., Nukleonika, 25, No. 10, 1197 (1980).
12. I. A. Golenishchev et al., Development of an Assembly of Equipment for Monitoring the Homogeneity of Mixed Oxide Fuel by the Method of α-Autoradiography, theses of Reports at the Ninth All-Union Scientific-Technical Conference on "Nondestructive Physical Methods and Means of Monitoring" [in Russian], Minsk (1981).

LIQUID-METAL TRANSDUCERS FOR EXAMINING THE DEFORMATION OF MATERIALS IN REACTOR EXPERIMENTS

V. A. Neverov and Yu. L. Revyakin

UDC 531.717

Deformation in a material, or in general small displacements, must be measured with high accuracy in various materials-science studies, such as in researching radiation swelling and creep. High accuracy is required in such measurements in order to provide reliable forecasting of fault-free operating periods for highly stressed components in the core of fast-neutron power reactors.

Scope for Using Existing Methods. In most existing devices used within reactors [1-3] for examining radiation creep, one measures the increments in the radial dimensions with the transducers placed axially in the zone where the neutron flux is less strong (10^{15}-10^{16} $m^{-2} \cdot sec^{-1}$). Therefore, any such system uses paired intermediate links (levers, ties, etc.), which convert the transverse displacements into longitudinal ones and transmit them to considerable distances. It is complicated to estimate the accuracy of readings from transducers coupled to such links, since one needs to know the actual temperature distribution along the paired ties, levers, and other elements as arising in variable local gas flows.

Also, the transfer links are subject to instability in the radiative energy deposition, which is affected by the automatic reactor-power control system [4], as well as by vibrations. The fluctuations in readings from transducers monitoring the core by means of paired links are particularly large when there are large gas gaps and considerable energy deposition, particularly at values more than $1\text{-}8 \times 10^3$ W/kg. In such cases, the fluctuations may attain 10-30 μm, which is equivalent to 0.2-0.4% strain in the specimens, which substantially complicates the interpretation or may even make the readings from high-sensitivity transducers of little practical use (ones with sensitivity of 0.01-0.005% of the specimen diameter). It is largely ineffective to use automatic compensation in the differences in thermal expansion [3] for highly loaded reactor channels, and it also reduces the useful volume in the cells.

Translated from Atomnaya Énergiya, Vol. 57, No. 5, pp. 349-353, November, 1984. Original article submitted October 28, 1983; revision submitted May 4, 1984.

 0038-531X/84/5705-0778$08.50

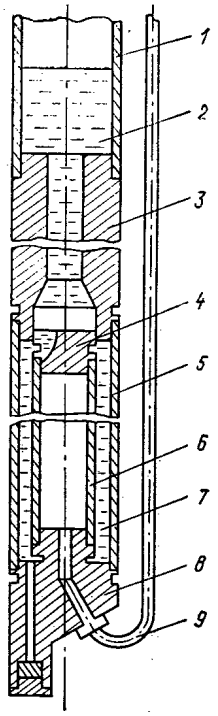

Fig. 1. Design of liquid-metal transducer: 1) measurement chamber; 2) liquid metal; 3) junction sleeve; 4) upper specimen plug; 5) ampoule; 6) specimen; 7) annular gap; 8) lower specimen plug; 9) gas loading line.

As a rule, the radial dimensions of the auxiliary units in such transducers are substantial [1-3, 5], and as a result one can only test a single specimen, which is inadequate for accelerated selective experiments.

Strain-gauge transducers as used in the IRT-2000 reactor [6] eliminate the destabilizing effect of the gas gaps. However, such transducers are unstable and do not have a long working life in intense fluxes of neutrons (up to 2×10^{19} $m^{-2} \cdot sec^{-1}$) and γ rays (up to 10^4 Gy/sec) such as are characteristic of fast reactors, and where the sodium coolant temperature may exceed 300°C. Acoustic transducers [5, 6] eliminate intermediate transfer links. However, they do not eliminate the destabilizing action of the gas gap between the specimen and the nozzle. Also, an acoustic nozzle in the central plane of the core alters the local power levels in the heat sources and sinks, and the perturbations in the temperature pattern along the height and perimeter of the specimens may be very substantial and may produce additional stresses in the specimen.

Features of Liquid-Metal Transducers. One can provide effective matching of the temperature conditions in the transfer links by using liquid-metal transducers. The liquid metal (Fig. 1) surrounds the entire side surface of the specimen, which is a thin-walled tube whose diameter and thickness are the same as those used for the fuel pins. The specimen is placed within an ampoule flushed on the outside by the reactor coolant, and the walls of the ampoule should be maximally relieved from mechanical stresses in order to ensure stable dimensions. The liquid metal is introduced from below into the annular gap between the walls of the specimen and the ampoule. Any increase in volume due to radiation creep or swelling gradually reduces the volume occupied by the liquid metal [7]. Therefore, the specimen acts on the surrounding liquid metal, which acts as the sensing element. The destabilizing gas gaps are completely eliminated, and one judges the volume change in the specimen from the level of the liquid metal in the measurement chamber placed at a suitable distance.

The specimen is loaded from within by gas pressure. The level shift in the measurement chamber should be recorded periodically when the initial temperatures have been attained throughout the height of the liquid-metal transducer. The secondary system tracking the liquid-metal level can employ any standard contactless method [1, 2, 5].

The metal used in the transducer should have a low melting point and low vapor pressure, as well as a low rate of corrosion interaction with the contacting surfaces, which it should not wet. It should also have a low activation cross section in order to minimize the conversion to other elements, particularly ones with very different density. The metal meeting these requirements best at 280-360°C is tin. One can also use gallium and indium, or the

lead–bismuth eutectic at higher temperatures. To reduce the effects of oxide films, the free volume of the transducer should be filled with inert gas. The effects of the surface tension in a liquid metal can be eliminated in designing the servo system.

This transducer can convert very small changes in radius (0.2-0.4 μm) into appreciable displacements (20-200 μm) in the liquid-metal column. The relationship between the two displacements is given by the following:

$$\Delta h = 0.01\,\bar{\varepsilon}_r\,L_0\,(2.5 + 0.02\,\bar{\varepsilon}_r)\,(\bar{d}_0/d_2)^2; \tag{1}$$

$$k_{tr} = \frac{\Delta h}{\Delta \bar{d}_0}, \tag{2}$$

where Δh is the response of the transducer to the volume deformation ε_V of the speciemn, $\bar{\varepsilon}_r = \overline{\Delta d_0}/\overline{d_0}$ is the radial proportion of the component averaged over the height of the working part expressed in %, $\bar{d}_0$ and L_0 are the initial values of the outside diameter and height of the working part, d_2 is the internal diameter of the measurement chamber, and k_{tr} is the coefficient for the conversion of Δd_0, the radial displacement of the side surface, into displacement of the liquid-metal column.

The tranducer response is taken as the level shift in the measurement chamber, which is reckoned from some initial value recorded before each fresh factor operates beginning when the device is placed in the reactor cell, namely: before the start of irradiation, before the loading with a given internal gas pressure, and so on. The initial and all subsequent levels are recorded at the same temperature, which is established from the initial readings E_0 of thermoelectric thermometers by varying the temperature of the incoming sodium coolant. The daily variations in this temperature do not usually exceed ± 10°C in fast reactors (±400 μV), and if necesary they can be eliminated for 1-2 h. An R-307 direct-current potentiometer is used to measure the thermo-emf. Measurements with the BOR-60 reactor indicate that a given temperature can be maintained for 20-30 min to ± 0.25°C (± 10 μV). This is sufficient to take repeated readings from the secondary system tracking the liquid-metal level. One can convert from the total bulk deformation ε_V to the radial deformation averaged over the height $\bar{\varepsilon}_r$ by means of (1). One can use the justified assumption [8] that the axial deformation ε_L and the radial one ε_r are related by the following for an isotropic thin-walled tube loaded by excess internal pressure:

$$\varepsilon_L = \frac{1}{2}\,\varepsilon_r. \tag{3}$$

This relationship can be checked and if necessary modified by examining the specimens after irradiation and recording profiles characterizing the deformation in various sections, in particular at the ends. The radial deformations averaged over the height

$$\bar{\varepsilon}_r = \frac{\int_l^0 \varepsilon_r(l)\,dl}{L} \tag{4}$$

and the measured elongations define the true relation for any particular material if $\varepsilon_r(l)$ is nonuniform. Such measurements and refinements essentially represent calibrating the liquid-metal transducer and allow one to make the necessary corrections to the measured $\bar{\varepsilon}_r$.

Choice of Transducer Sensitivity and Working Characteristics. It follows from (1) that one can attain a given response to deformation by choosing the three independent parameters $\bar{d}_0$, L, and d_2. A liquid-metal tranducer sums the radial deformations in all sections, whereas other transducers [1-3, 5, 6] record only the deformation in one section. The dependence of Δh on the diameter is quadratic, whereas that on the length is linear, which gives particular significance to the tubular shape of the specimen on adjusting the system to record the deformations, and correct choice of specimen dimensions provides for better results on the radiation response of reactor materials. For example, if $\bar{\varepsilon}_r$ is 1% during a reactor experiment, then with $\Delta \bar{d}_0$ = 70 μm we have for a tubular specimen with d_0 = 7 mm and L_0 = 400 mm that $\Delta h'$ = 6.1 mm and $\Delta h''$ = 31 mm, with transformation coefficients k'_{tr} = 87 and k''_{tr} = 441 for diameters of the measurement chamber d'_2 = 9 mm and d''_2 = 4 mm correspondingly. Increasing the specimen diameter to d'''_0 = 9 mm enables one to raise the response to $\Delta h'''$ = 51 mm and the transformation coefficient to k'''_{tr} = 567 for d_2 = 4 mm.

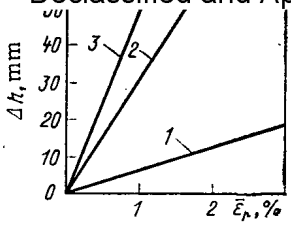

Fig. 2. Dependence of liquid-metal level shift Δh in the measurement chamber on radial deformation $\bar{\varepsilon}_r$ for tubular specimens: 1) k_{tr} = 87; d_o = 7 mm; L_o = 400 mm; d_2 = 9 mm; 2) k_{tr} = 441; d_o = 7 mm; L_o = 400 mm; d_2 = 4 mm; 3) k_{tr} = 567; d_o = 9 mm; L_o = 400 mm; d_2 = 4 mm.

Exact measurement of the initial parameters d_o, L_o, and d_2 enables one to avoid preliminary calibration if (3) is obeyed, which substantially simplifies the use of such transducers. One can calculate the rise in the metal in the measurement chamber in response to Δd_o and ΔL_o. One converts from these absolute deformations to the relative ones $\varepsilon_r = \Delta d_o/d_o$ and $\varepsilon_L = \Delta L_o/L_o$ corrected by reference to control measurements in a shielded chamber to identify the proportion of each of them by means of equations analogous to (3). Figure 2 gives the working characteristics of the above transducers with k_{tr} of 87, 441, and 567. These characteristics enable one to convert Δh as determined by the tracking system to $\bar{\varepsilon}_r$. Measurements are made at actual times $\tau_1, \tau_2, \ldots, \tau_n$ of the values $\bar{\varepsilon}_r(\tau_1), \bar{\varepsilon}_r(\tau_2), \ldots, \bar{\varepsilon}_r(\tau_n)$, which characterize the deformation dynamics in any section, since the relative contributions from each of them to the overall deformation $\varepsilon_V(\tau_1), \varepsilon_V(\tau_2), \ldots, \varepsilon_V(\tau_n)$ remain unchanged. This implies that one attains a $\bar{\varepsilon}_r = f(\tau)$ relationship, or in the general case $\varepsilon_V = f(\tau)$, which enables one to determine the creep parameters and the swelling rate.

Features of a Reactor Device Fitted with a Liquid-Metal Transducer. The above typical dimensions of major elements have been used in the TO-IRP device for examining radiation creep in tubular specimens placed in ampules containing liquid metal in the BOR-60 reactor. The ampules were cooled by the sodium coolant entering from the pressurized collector. The temperature rise within the working part of the device of length 700 mm was not more than 2-3°C. The bodies of the transducers were closely thermostatted (ΔT= ± 0.25-1.0°C at the time of measurement) by increasing the coolant flowrate to 2 m^3/h (with a total heat production $Q \approx 2$ kW) and by the use of an insulating gas gap around the body of the TO-IRP, which reduced the heat influx from adjacent pin sets by more than a factor 10. The device is compact, which means that up to seven specimens can be located in a cell of diameter 44 mm in the core of the BOR-60, where the liquid-metal transducers are fitted with servo systems having acoustic [5] or electrical-contact level transducers.

The viability of these liquid-metal transducers was tested before starting up the reactor by varying the temperature within limits of ± 25°C and then restoring the previous value by reference to thermocouple readings with an accuracy of 0.25°C with the maximum coolant flowrate (∿ $2 m^3/h$). The coolant temperature was varied by electrical heaters on the supply pipes. When the previous value was restored, the readings of the tracking system were restored with an error of not more than 5-10 μm, which is equivalent to $\bar{\varepsilon}_r$ = 0.002% (for a diameter of 6.9 mm). For practical purposes, the measurement accuracy may be taken as $\Delta\bar{\varepsilon}_r \approx \pm$ 0.01%, and then the permissible error in controlling the temperature for 20-30 min is 1-2°C, which is quite possible with any reactor.

The sensitivity with a liquid-metal transducer and acoustic device is 0.1-0.8 μm. In some cases, the error of measurement was 1-1.5% for 1% deformations in specimens of diameter 6.9 mm and wall thickness 0.4 mm ($\Delta\bar{d}_o$ = 69 μm) because of the strict temperature stabilization, and it never exceeded ± 4% in any of the experiments.

Results of Tubular Specimen Deformation. The TO-IRP was used in examining the deformation of the common steel OKh16N15M3B [7] to check the viability of this transducer in the BOR-60 reactor. We used tubular specimens of diameter 6.9 mm with wall thickness 0.4 mm. The deformation was produced at 320 ± 5°C with a stress of 197 MPa referred to the uniaxial state. The specimens were under load for 1613 h. Up to that time, the fast-neutron fluence was 9.3×10^{25} m^{-2} ($E_n > 0.1$ MeV). The neutron flux at the center was not more than 2×10^{19} $m^{-2} \cdot sec^{-1}$ with a nonuniformity factor K_Z = 1.12. The damaging dose in the central section was 4.4 displacement/atom (from the TRN standard model). Figure 3 shows the creep curve. At 190 h after the start of loading, steady-state creep set in, and the creep rate and modulus for this steel were as follows on the basis of the $\bar{\varepsilon}_{rII}$ deformation and the damaging dose of 4.0 displacement/atom acquired during the last 1420 h of test: $\dot{\bar{\varepsilon}}_{II} = (24 \pm 1) \cdot 10^{-5}$ %/h and $B = (4.4 \pm 0.8) \cdot 10^{-6}$ (MPa·displacement/atom)$^{-1}$. Then $\bar{\varepsilon}_r$ was 0.62%, with 0.2% obtained during the first creep stage.

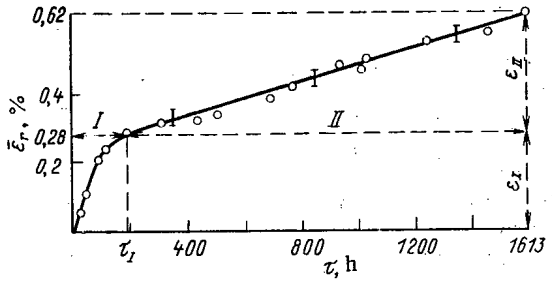

Fig. 3. Radiation-creep curve for 0Kh16N15M3B steel at 320 ± 5°C and a load of 197 MPa recorded with the liquid-metal transducer and acoustic device: O) experiment; I and II) stages of transient and steady-state creep.

There are 15-20% differences between these values and the measurements of [7] on the deformation of specimens previously irradiated to 30-40 displacement/atom, which shows that the TO-IRP gives reliable data.

This liquid-metal tranducer has satisfactory thermal and radiation resistance, together with high sensitivity, compactness, and reliability, and these devices can be recommended for testing the deformation of materials in reactors at 300-340°C at mechanical stresses up to 500 MPa with fast-neutron fluxes up to 2×10^{19} $m^{-2} \cdot sec^{-1}$ and radiative energy deposition up to 6×10^3 W/kg.

LITERATURE CITED

1. D. Wood, J. Nucl. Mater., 65, 329-335 (1977).
2. H. Hafner, Atomwirtschaft, No. 7, 359 (1974).
3. V. N. Kiselevskii, N. P. Losev, V. K. Lukashov, et al., Mechanical Test Methods for Materials under Irradiation: A Study of Reactor Materials with Deformation Measurement [in Russian], NIIAR Preprint P-249, Dimitrovgrad (1974).
4. V. A. Tsykanov and B. V. Samsonov, Techniques for Irradiating Materials in High-Flux Reactors [in Russian], Atomizdat, Moscow (1973), p. 262.
5. A. V. Zelenchuk and K. V. Naboichenko, "An acoustic method of measuring small displacements at high temperatures in radiation fields," At. Energ., 36, No. 2, 130-132 (1974).
6. A. V. Zelenchuk, B. V. Fetisov, Yu. G. Lakin, and V.Yu. Tonkov, "Methods of measuring the deformation in fuel-pin sheaths during irradiation," At. Energ., 44, No. 6, 505-508 (1978).
7. V. A. Krasnoselov, A. N. Kolesnikov, V. I. Prokhorov, et al., An Experimental Study of Radiation Creep in Stainless Steels [in Russian], NIIAR Preprint 16 (469), Dimitrovgrad (1981).
8. G. S. Pisarenko, A. P. Yakovlev, and V. V. Matveev, Handbook on Material Resistance [in Russian], Naukova Dumka, Kiev (1975), p. 704.

RADIATION CHANGES OF THE PROPERTIES OF CARBON PYROCERAMIC

Yu. S. Virgil'ev and E. I. Kurolenkin

UDC 621.039.532.21

Carbon pyroceramics [1], in view of the special features of their structure and properties, are being considered as a prospective material for thermonuclear reactors [2]. Because of this, a study of its radiation properties will be of practical interest, as the published data [3] are insufficiently complete.

In the present paper, the results are given of an investigation of the radiation changes of structure and properties of carbon pyroceramic (CPC), including being subjected to additional thermal treatment in argon and *in vacuo* (~ 0.1 Pa) at a temperature of 1400-3000°K. Irradiation of the CPC samples was conducted in the core of a research water-cooled/water-moderated reactor at a temperature from 320-340 up to 1000-1030°K and up to a neutron fluence of $2.5 \cdot 10^{21}$ cm^{-2} ($E \geqslant 0.18$ MeV).

Before and after irradiation, the following were measured: density (d_k), specific electrical resistance ρ, thermal conductivity at room temperature λ, coefficient of thermal expansion α in the range 300-800°K, dynamic modulus of elesticity E, breaking strength with bending σ_b and compression σ_c, microhardness H_v, geometrical dimensions, and also the parameters of the crystal lattice c and a, dimensions of the region of coherent scattering, structural porosity ε [4] and intensity of the small angle x-ray scattering for $\varphi = 30'$, characterizing the specific surface of the boundaries of the structural pores. The measurements were made by the accepted methods (see, for example, [5]).

It is known [1] that the supermolecular arrangement of CPC determines the isotropic or pseudoisotropic spherical particles of carbon, formed during synthesis, and which are characterized — just like glass-carbon materials [6] — by the structural porosity, which is a consequence of incomplete packing of the crystal intergrowths. This porosity amounts to 25% of the total porosity of the material. The pseudoisotropic particles of CPC form quite extended structural complexes — clusters. Their packing density is defined by the microporosity which makes the predominant contribution to the total porosity of CPC. Highly orientated (pyrographite) structures can be formed during synthesis on the sufficiently developed surface of these complexes. The definite anisotropy and fluctuations of the physical properties, which vary with neutron irradiation (see Table 1), are the consequence of this structural arrangement of CPC.

TABLE 1. Mean Arithmetic Deviation from the Average Value of Certain Parameters of Carbon Pyroceramic, Thermally Processed at 2100°K before and after Irradiation, %

State	ρ	E	α	I*
Before irradiation	6,0	4,5	3,6	12,2
After irradiation†	12,2	21,7	2,8	4,9

*I is the intensity of the small-angle x-ray scattering.

†Irradiation at 770°K up to a fluence of $1.6 \cdot 10^{20}$ cm^{-2} ($E \geqslant 0.18$ MeV).

Translated from Atomnaya Énergiya, Vol. 57, No. 3, pp. 353-356, November, 1984. Original article submitted December 29, 1983.

0038-531X/84/5705-0783$08.50

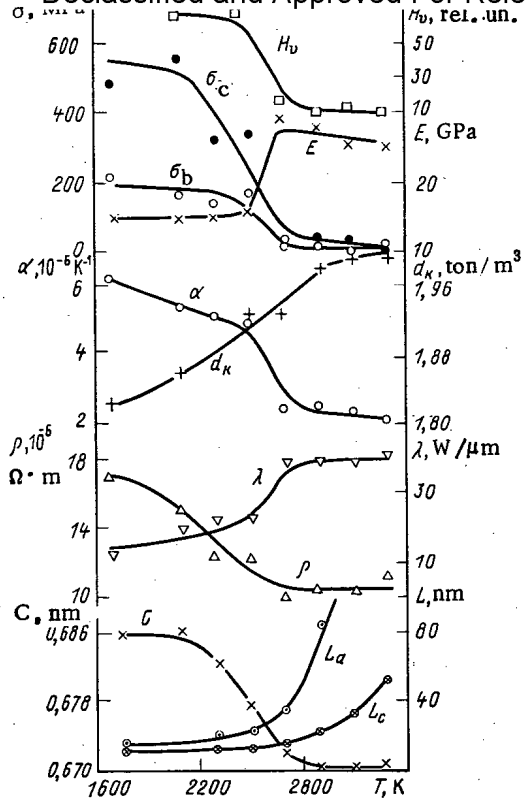

Fig. 1. Effect of the processing temperature of carbon pyroceramic CPC *in vacuo* on the crystal lattice parameter c; diameter L_a and height L_c of the region of coherent scattering; the specific electrical resistance ρ; thermal conductivity λ; coefficient of thermal expansion α; density d_k; breaking strength for compression σ_c and bending σ_b; modulus of elasticity E, and microhardness H_V.

The change of physical properties of CPC after thermal processing *in vacuo* is illustrated in Fig. 1, whence it can be seen that above 2500°K intensive graphitization takes place. Above 2800°K, the material is graphitized completely; judging by the lattice parameter c, it becomes even "more perfect" than Ceylon graphite, used as a standard for x-ray films. The diameter and height of the CPC crystals at this temperature exceed 10 nm.

Reorganization of the CPC structure as a result of graphitization is accompanied by a reorganization of its supermolecular arrangement. After thermal treatment at 2500°K the globules disappear, coarse formations appear — dendrites, which at the higher temperature grow into quite large (up to several millimeters in cross section), platelike regions disorientated relative to one another, forming the granular structure of the CPC. The mutual intergrowth of the dendrites creates a dense (d_k = 1.9-2.1 tons/m^3) structure of the CPC, impenetrable for gas—liquid media.

During graphitization, redistribution of the porosity also takes place. The structural porosity ε increases up to 2300°K and then rapidly decreases, amounting to a total of 0.32% at 2700°K, whilst the microporosity Π remains almost constant [6]. It is shown below how the porosity varies as a function of the temperature of processing, %:

	ε	Π
1700 K	3,20	11,6
2300 K	5,40	9,2
2500 K	4,90	9,4
2700 K	0,32	11,0
2900 K	0,24	10,2
3300 K	0,11	11,8

The change of structure of CPC as a result of thermal processing corresponds to the change of its physical properties and especially the porosity, which after thermal processing at 2500-2800°K is reduced by a factor of approximately 10. It should be noted that the ratio of the breaking strengths for compression and bending, equal to 2.4 for the original CPC (this is characteristic for a brittle material), after thermal processing at a temperature above 3000°K becomes close to unity, as for metals.

The deformation ε_d, calculated from the values of the breaking strength on bending and the dynamic modulus of elasticity, is significantly higher for CPC than for other carbon materials.

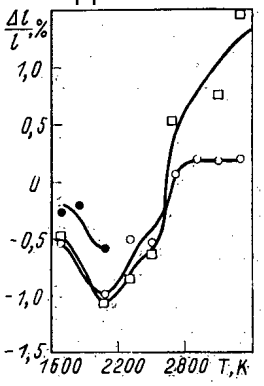

Fig. 2

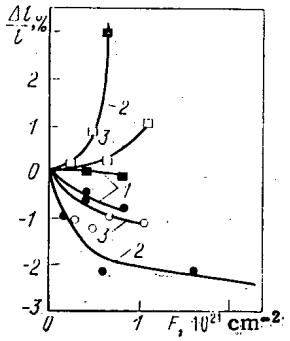

Fig. 3

Fig. 2. Dependence of the relative change of length of CPC samples on the temperature of their treatment in argon (●) and *in vacuo* ∿ 0.1 Pa (○). Irradiation at a temperature of 1000-1100°K up to a neutron fluence of $4 \cdot 10^{20}$ (●); $6.5 \cdot 10^{20}$ (○), and $10.5 \cdot 10^{20}$ cm^{-2} (□).

Fig. 3. Dependence on the neutron fluence of the relative change of length of CPC samples thermally treated at 2100°K (○, ●) and at 3100°K (□, ■) *in vacuo* (□, ○)) and in argon (●, ■). Irradiation temperature 670 (1), 770-820 (2) and 1000-1100°K (3).

The values of the deformation for different carbon materials are shown below, %:

CPC	1,4—1,5
MPG-6	0,50
ZOPG	0,31
PROG-2400	0,20—0,23
SG-P	0,08

Thermal processing of CPC at a temperature above 2500°K sharply reduces the deformation ε_d, which for completely graphitized samples is equal to the deformation of silicified graphite grade SG-P.

The irradiation of samples of CPC at 340°K causes their growth, so that for $F < 10^{20}$ cm^{-2} the samples break down completely. For samples of CPC irradiated at 570°K up to a neutron fluence of $3.7 \cdot 10^{30}$ cm^{-2} (sic), the end boundaries were slightly carbonized, but the samples themselves were bent strongly. A layered structure of the material developed which can be seen clearly with the more perfect highly orientated samples: the layers were arranged parallel to the plane of deposition of the CPC. In this case, a change of the structural characteristics of CPC was observed, typical for carbonaceous materials — a reduction of the crystal lattice parameter a, and also the height (L_c) and diameter (L_a) of the region of coherent scattering. It is noteworthy that the parameter c for slightly graphitized samples does not increase during irradiation, but decreases and the ratio $\Delta c/c$ only becomes positive with increase of the degree of graphitization. It is shown below how $\Delta c/c$ varies as a function of the treatment temperature, %:

1700 K	−0,37
2100 K	−0,50
2300 K	−0,09
2700 K	−0,70
2900 K	−0,75

This reduction of the parameter c with irradiation cannot be caused by an improvement of the crystal structure of the CPC, as other structural characteristics are worsened. Evidently, here a relaxation of the internal stresses is observed, the level of which decreases with increase of the treatment temperature of the CPC. In fact, an investigation of the microhardness on a macrograin of CPC (models of macroparticles connected by self-adhesion, determining its globular structure) shows that thermal treatment up to 2100°K leads to a radistribution and equalizing of H_v over the cross section of the macrograin.

A further increase of the irradiation temperature of CPC reduces the radiation effects: samples irradiated at 670°K retain their external form. Shrinkage is increased with increase of the treatment temperature of the material, i.e., with increase of the degree of perfection of the crystal structure. Irradiation at 77°K and above causes the maximum shrinkage of samples treated at 2100°K. At a higher treatment temperature, shrinkage decreases sharply and then is replaced by swelling. Shrinkage of the samples with an imperfect structure increases with the neutron fluence (Fig. 2).

The data presented and also that obtained earlier [3, 6], allowed the dose curves of the relative change of length of CPC samples, thermally treated at 2100°K (with maximum shrinkage) and at 3100°K (with maximum swelling), to be constructed. It can be seen in Fig. 3 that the thermal treatment conditions (in argon and *in vacuo*) do not affect the change of shape of CPC samples. For nongraphitized samples (treated at 2100°K, degree of graphitization 0.01), the rate of shrinkage, which is very high at first, rapidly decreases with increase of the fluence, and then remains constant. Thus, during irradiation at 700-820°K, the rate of shrinkage relative to a neutron fluence of 10^{20} cm^{-2} at first attains 0.7% and then decreases by a factor of 11 to 0.06%, i.e., it approaches the rate of shrinkage of semifinished reactor graphite, thermally treated at the same temperature (2100°K) [7]. Thus, it is clear that with increase of the irradiation temperature the swelling of poorly finished samples of CPC changes to shrinkage, the rate of which reaches a maximum in the range 700-800°K and at 1100°K approximately it is close to zero.

During irradiation at 670°K, CPC samples thermally treated at 3100°K, undergo small shrinkage (see Fig. 3). For irradiation at 770-820°K, a high rate of growth of the samples is characteristic, as with secondary swelling of normal highly finished reactor graphite, but with low values of the neutron fluence (approximately by a factor of 10). With increase of the irradiation temperature up to 1000-1100°K, intense growth of the samples starts at higher values of the neutron fluence and takes place at a lower rate. Thus, in proportion with increase of the irradiation temperature, swelling of highly finished samples of CPC is replaced by shrinkage, after which intense secondary swelling follows. The finished material differs significantly in the small shrinkage from the nongraphitized CPC considered earlier.

The nature of the change of properties of CPC samples as a result of irradiation depends on the thermal treatment temperature. For the initial nongraphitized samples of CPC (1700°K), no changes of the specific electrical resistance, like, for example, nongraphitized semifinished reactor graphite [7], would be expected. However (Fig. 4), the ratio $\Delta\rho/\rho$ is not equal

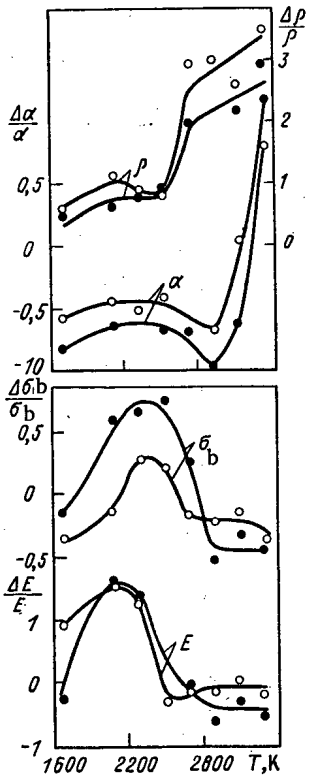

Fig. 4. Dependence of the relative change of the modulus of elasticity E; breaking strength on bending σ_b; coefficient of thermal expansion α, and specific electrical resistance ρ on the treatment temperature of CPC *in vacuo*. Irradiation at a temperature of 770-820 (○) and 1000-1100°K (●) respectively until reaching a neutron fluence of $6.5\cdot10^{20}$ and $10.5\cdot10^{20}$ cm^{-2}.

to zero but increases with increase of the treatment temperature, which is related with an improvement of the crystal structure of the material. A particularly sharp increase of $\Delta\rho/\rho$ is observed for CPC samples thermally treated at a temperature in excess of 2700°K, i.e., having the greatest degree of perfection.

Not only the degree of imperfection of the crystal lattice has a considerable effect on the change of electrical resistance as a result of irradiation, but also the mutual interaction of the supermolecular arrangement. Weakening of this interaction with increase of the treatment temperature leads to a more intense breakdown of the structure and to the development of porosity as a result of irradiation and, consequently, also to a stronger increase of the electrical resistance.

It is shown below how, as a result of the irradiation of CPC samples at 810°K up to a neturon fluence of $5.3 \cdot 10^{20}$ cm^{-2} and using the method of small-angle x-ray scattering, the structural porosity and microporosity varies as a function of the treatment temperature %:

	$\Delta\varepsilon/\varepsilon$	$\Delta\Pi/\Pi$
2500 K . . .	—39	—2
2700 K . . .	43	0
2900 K . . .	40	2
3100 K . . .	135	28

The change of the modulus of elasticity and strength by irradiation of CPC at a different treatment temperature occurs nonmonotonically (see (Fig. 4). Both the original samples and those treated above 2500°K are weakened during irradiation. At the same time, the ratio of the breaking strengths under compression and bending is almost unchanged, and the deformation of samples thermally treated up to 2200°K decreases even more strongly than below the irradiation temperature. The deformation of graphitized CPC samples is unchanged.

The complex nature of the radiation changes of properties of CPC with a different treatment temperature can be explained by the simultaneous action of several factors, and each predominates in a defined treatment temperature range of the material. Thus, for nongraphitized CPC (thermal treatment at a temperature up to 2100°K) the determining factor evidently is the internal stresses, decreasing with increase of the treatment temperature. High stresses promote the development of microcracks [6] and a corresponding decrease of strength of the material on irradiation.

Graphitized samples of CPC (thermal treatment at a temperature above 2600-2800°K) are subject to secondary swelling, started during irradiation almost immediately, so that there is no shrinkage. Secondary swelling, as it is well known, is accompanied by the intense development of microcracks, which leads to a reduction of strength and to an anomalously high increase of the specific electrical resistance.

Thus, thermal treatment above 2500°K causes intense graphitization of CPC, which is almost completely concluded at 2700°K. Samples of nongraphitized CPC undergo shrinkage during irradiation at a temperature above 500-600°K. The rate of shrinkage is slowed down with increase of the neutron fluence, and its level is reduced with increase of the irradiation temperature. With graphitized CPC, swelling is observed, which decreases with decrease of the irradiation temperature. Irradiation of both nongraphitized and completely graphitized samples of CPC leads to their weakening, accompanied by an anomalously high increase of the specific electrical resistance because of the intense development of microcracks.

LITERATURE CITED

1. G. M. Volkov, V. I. Kalugin, L. A. Plautalova, and A. M. Sigarev, "Carbon pyroceramics — a new class of carbon materials," in: Properties and Application of Antifriction Self-Lubricating Materials [in Russian], TsNIItsvetmetinformatsiya, Moscow (1970), p. 107.
2. N. V. Pleshivtsev, Yu. S. Virgil'ev, G. M. Volkov, et al., "Physicochemical, mechanical and vacuum properties of carbon pyroceramic and erosion of its surface during bombardment with hydrogen and helium ions," Fiz. Khim. Obrab. Mater., No. 6, 30-39 (1981).
3. Yu. S. Virgil'ev, G. M. Volkov, E. N. Zakharova, et al., "Radiation dimensional stability of carbon pyroceramic," in: Structural Materials Based on Carbon [in Russian], Metallurgiya, Moscow, XI (1976), pp. 68-74.
4. E. I. Kurolenkin and Yu. S. Virgil'ev, "Investigation of the supermolecular structure of carbon materials," Khimiya Tverd. Topliva, No. 5, 77-86 (1980).

5. V. V. Goncharov, N. S. Burdakov, Yu. S. Virgil'ev, et al., Action of Irradiation on the Graphite of Nuclear Reactors [in Russian], Atomizdat, Moscow (1978), p. 272.
6. E. I. Kurolenkin, G. M. Butyrin, and Yu. S. Virgil'ev, "Gas permeability and change of samples of glass carbon and carbon pyroceramic during irradiation with neutrons," Izv. Akad. Nauk SSSR, Ser. Neorgan. Mater., 18, No. 2, 308-312 (1982).
7. P. A. Platonov, I. F. Novobratskaya, Yu. P. Tumanov, and V. I. Karpukhin, "Effect of the degree of perfection of graphite on the change of its properties during irradiation," At. Energ., 46, No. 4, 248-254 (1979).

SPONTANEOUS FISSION HALF-LIFE OF ^{240}Pu

A. A. Androsenko, P. A. Androsenko,
Yu. V. Ivanov, A. E. Konyaev,
V. F. Kositsyn, É. M. Tsenter,
and V. T. Shchebolev

UDC 549.799:539.125.5

In the development of nuclear physics methods of analysis and monitoring of fissionable materials by neutron self-radiation, and also in the creation of a metrological guarantee of these methods, an increase in the accuracy of data on spontaneous fission half-lives T_{sf} of the main transactinium nuclides is of major importance [1-5]. For most spontaneously fissionable nuclides T_{sf} is known to a few percent [1-5]. However, according to data in [1-17], T_{sf}^{240} for ^{240}Pu, which has an appreciable specific flux of spontaneous fission neutrons, N_{sf}^{240}, lies in the range from 1.15×10^{11} yr [5, 14] to 1.45×10^{11} yr [11].

Most of the experimental data were obtained from direct fission fragment counting by ionization chambers or gas-filled scintillation counters. While this method has become classical, it is not without intrinsic shortcomings. These include the difficulties of an accurate determination of the mass ($\sim$ 1mg) of a small plutonium sample, taking account of absorption and scattering of fission fragments by nuclei of materials of the weighed sample and backing, the necessity of using nanosecond electronics to eliminate spurious pulses arising as a result of the superposition of background pulses from alpha particles, which may contribute as many as 10^7 counts per sec. These clearly account for the considerable spread of the results obtained.

The method based on a measurement of the integrated neutron flux from samples of known isotopic and chemical composition, mass, and shape does not have these disadvantages. The value of T_{sf}^{240} is determined by a subsequent calculation, taking account of ν_{sf}^{240} (the average number of neutrons produced per spontaneous fission of ^{240}Pu), the contribution of neutrons produced in the (α, n) reaction on the light impurity elements, neutrons from the spontaneous fission of other nuclides, and the effect of multiplication in the neutron self-field of the samples under study. We known of only one [15] article devoted to the determination of T_{sf}^{240} by this method. The value obtained was $T_{sf}^{240} = (1.170 \pm 0.025) \times 10^{11}$ yr.

Both the experimental [14-17] and estimated [1-5] values of T_{sf}^{240} obtained in recent years tend to decrease. For example, the authors of [16-17], published within a year of one another, used values of N_{sf}^{240} equal to 985 and 1022/g·sec, which corresponds to $T_{sf}^{240} = 1.20 \times 10^{11}$ and 1.15×10^{11} yr (for $\nu_{sf}^{240} = 2.14$ [16, 17]). At the same time, Khol'nov et al. [2] recommend the estimated value $(1.27 \pm 0.04) \times 10^{11}$ yr.

In the present article we report on the determination of T_{sf}^{240} from measured values of neutron fluxes from two spherical plutonium samples with a high ^{240}Pu content. The neutron flux Y from such samples is

$$Y = Y_{sf} + Y_{\alpha n} = K_{sf} \overline{N}_{sf} M + K_{\alpha n} \overline{N}_{\alpha n} M, \quad (1)$$

where Y_{sf} and $Y_{\alpha n}$ are, respectively, the neutron fluxes from spontaneous fission and from the (α, n) reaction on light admixtures, K_{sf} and $K_{\alpha n}$ are the multiplication factors of neu-

Translated from Atomnaya Énergiya, Vol. 57, No. 5, pp. 357-359, November, 1984. Original article submitted December 5, 1983; revision submitted April 19, 1984.

 0038-531X/84/5705-0788$08.50

trons from spontaneous fission and the (α, n) reaction, $\bar{N}_{sf}$ and $\bar{N}_{\alpha n}$ are the specific neutron fluxes from spontaneous fission and the (α, n) reaction averaged over the isotopic and chemical composition, and M is the mass of the sample.

The neutron fluxes from samples SP-1 and SP-2 investigated were measured with equipment of the State Primary Neutron Flux Standard at the D. N. Mendeleev All-Union Instrument Research Institute of Metrology, and were 8.655×10^4/sec and 4.23×10^4/sec. The relative errors of the measured values for a 0.95 confidence coefficient were 1.4% and 2%, respectively. The masses of the samples investigated were 82.93 g and 41.46 g, with an error of ± 0.01 g, and the density of the material was 17.10 g/cm^3, with a relative error of 0.2%. The isotopic composition of the plutonium in % was as follows: ^{238}Pu $< 10^{-4}$; ^{239}Pu 7.71 ± 0.01; ^{240}Pu 89.33 ± 0.0.1; ^{241}Pu 2.79 ± 0.01; ^{242}Pu 0.17 ± 0.01.

Neutrons from the (α, n) reaction, even for a small concentration of admixtures, can make an appreciable contribution to the total flux. The average neutron flux per α particle from the (α, n) reaction in a mixture of isotopes is [18]:

$$\bar{y}_{\alpha n} = \frac{\sum_i y_i C_i S_i / M_i}{\sum_i C_i S_i / M_i}, \qquad (2)$$

where y_i is the neutron flux per α particle from the (α, n) reaction on the i-th element of the mixture, C_i is the mass concentration of the i-th element, S_i is the relative stopping power of the i-th element, and M_i is the atomic mass of the i-th element of the mixture.

The specific neutron flux from the (α, n) reaction is

$$\bar{N}_{\alpha n} = \sum_j N_{\alpha j} \bar{y}_{\alpha j}, \qquad (3)$$

where $N_{\alpha j}$ is the specific α activity of the j-th nuclide.

Aside from the plutonium isotopes, the only transactinium nuclide present in the sample in an appreciable amount is ^{241}Am, which is formed in the decay of ^{241}Pu ($T_{1/2}$ = 14.64 yr [2]). The mass content of ^{241}Am at the time of measurement of the neutron fluxes was determined by γ spectroscopy to be ∿ 1.1% of the total plutonium mass. The measured values are in good agreement with the values calculated by assuming that there was no ^{241}Am at the time the sources were prepared.

The values of the specific α activity and the average energy of the α particles from the plutonium isotopes and ^{241}Am were taken from [2], and the values of the average neutron fluxes from (α, n) reactions on impurity elements and the relative stopping powers were taken from [19] and [20], respectively. The calculated value of $\bar{N}_{\alpha n}$ was 10.0 ± 1.0/sec·g, while the total spectrum of neutrons from the (α, n) reaction has an average energy ∿ 2 MeV, and is negligibly different from the fission neutron spectrum [17, 20, 21]. The specific neutron flux from spontaneous fission $\bar{N}_{sf}$ is made up of N_{sf}^{240} and N_{sf}^{Σ}, where N_{sf}^{Σ} is the sum of the contributions of the other spontaneously fissionable nuclides present in the samples. The latter, determined mainly by the ^{242}Pu contribution and by using estimated constants from [2], was 2.9 ± 0.1/sec·g.

The multiplication factors were calculated by using an adaptation of BRAND — a complex of programs for modeling neutron physics experiments by the Monte Carlo method [22]. Since $\bar{N}_{\alpha n}$ is less than 1% of N_{sf}, and the spectrum of neutrons from the (α, n) reaction is negligibly different from the fission spectrum, we can take

$$K_{\alpha n} = K_{sf} = K_y \qquad (4)$$

practically without losing accuracy in the estimation of T_{sf}^{240}.

K_y was calculated by using the BNAB-78 [23] multigroup constants. According to estimates of the authors, the error of the calculation of k_{eff} for a large plutonium assembly is 1.4% [23, 34]. In the first approximation K_y is related to k_{eff} by the equation

$$K_y = \frac{1}{1 - k_{eff}}. \qquad (5)$$

TABLE 1. Values of Multiplication Factors of Samples

Sample	K_y (BRAND)	K_y (MSA)
SP-1	1,095±0,015	1,092±0,020
SP-2	1,124±0,015	1,121±0,026

Consequently, their errors are given by the equation

$$\frac{\Delta K_y}{K_y} = (K_y - 1)\frac{\Delta k_{eff}}{k_{eff}} \quad (6)$$

and one can expect that the systematic component of the error of K_y calculated by using the BNAB-78 library is less than 0.5%.

The values of K_y were also calculated by the method of successive approximation (MSA) [25]. The results are in good agreement with the values obtained by the Monte Carlo method (Table 1). Using directly measured values of Y and calculated values of $\bar{N}_{\alpha n}$, N^{Σ}_{sf}, and K_y (BRAND), N^{240}_{sf} was found to be equal to $(1.03 \pm 0.03) \times 10^3$/sec·g for both samples. The value of ν^{240}_{sf} is known rather accurately [2-5]. We took $\nu^{240}_{sf} = 2.151 \pm 0.026$ [5], since this value was recommended by IAEA, and does not contradict other estimates [1-4].

Our value of T^{240}_{sf} is equal to $(1.15 \pm 0.03) \times 10^{11}$ yr. It agrees with the experimental value in [14], and with the estimate in [5]; it is close to the value $(1.170 \pm 0.025) \times 10^{11}$ yr from [15], but is substantially smaller than the value $(1.27 \pm 0.04) \times 10^{11}$ yr recommended in [2].

LITERATURE CITED

1. N. S. Shimanskaya, Nuclear Constants of Transactinium Isotopes of the Fuel Cycle [in Russian], V. G. Khlopin Radium Institute, Leningrad (1978), p. 22.
2. Yu. V. Khol'nov, V. P. Chechev, Sh. V. Kamynov, et al., Characteristics of the Radiations of Radioactive Nuclides Used in the National Economy [in Russian], Atomizdat, Moscow (1980), p. 375.
3. S. Raman, Transactinium Isotopes Nuclear Data, Vol. 3, IAEA, Vienna (1976), p. 39.
4. D. Muir, World Request List for Nuclear Data, Wrenda 79/80, INDS (SEC)-73URSF, IAEA, Vienna (1979).
5. A. Nichols and M. James, INDC(NDS)-126/NE, Summary Report IAEA, Vienna (1981), p. 17.
6. E. Kinderman, HW-27660 (1953).
7. F. Barclay, W. Galbraitl, K. Glover, et al., in: Proc. Phys. Soc. London, 67A, 646 (1954).
8. O. Chamberlane, G. Farwell, and E. Segre, Phys. Rev., 94, 156 (1954).
9. V. L. Mikheev, N. K. Skobeev, and G. N. Flerov, Zh. Eksp. Teor. Fiz., 37, 59 (1959).
10. D. Watt. F. Bannister, J. Laidler, et al., Phys. Rev., 126, 264 (1962).
11. L. Z. Malkin et al., At. Energ., 15, No. 2, 158 (1963).
12. J. Perkin, P. White, and P. Fieldhouse, J. Nucl. Energy, 19, 423 (1965).
13. P. White, J. Nucl. Energy, 19, 323 (1965).
14. C. Budtz-Jorgensen and H. Knitter, "Neutron-induced fission cross section of ^{240}Pu in the energy range from 10 keV to 10 MeV."*
15. P. Fieldhouse, D.Malther, and E. Culliford, "The spontaneous fission half-life of ^{240}Pu," J. Nucl. Energy, 21, 749 (1967).
16. N. Ensslin, M. Evans, H. Menlove, et al., "Neutron coincidence counters for plutonium measurements," Nucl. Mater. Management, 7, 43 (1978).
17. N. Ensslin, J. Steward, and J. Sapiv, "Self-multiplication correction factors for neutron coincidence counting," Nucl. Mater. Management, 8, 60 (1979).
18. E. M. Tsenter, "Dependence of reaction yields under the action of α particles on the composition of the bombarded samples," Izv. Akad. Nauk SSSR, Ser. Metall. Toplivo, No. 1, 159 (1961).

*Journal citation missing in Russian original — Publisher.

19. H. Liskien and A. Poulsen, "Neutron yields of light elements under α-particle bombardment," Atomkernergie, 8, 28 (1977).
20. G. V. Gorshkov et al., Natural Neutron Background of the Atmosphere and Earth's Crust [in Russian], Atomizdat, Moscow (1966).
21. M. A. Bak and N. S. Shimanskaya, Neutron Sources [in Russian] Atomizdat, Moscow (1969).
22. P. A. Androsenko and A. A. Androsenko, "Possibilities of the set of BRAND programs for modeling neutron physical experiments by the Monte Carlo method," Preprint FÉI-1300, Obninsk (1982).
23. L. P. Abagyan et al., Group Constants for Reactor and Shield Calculations [in Russian], Énergoizdat, Moscow (1981).
23. L. P. Abagyan et al., At. Energ., 4, No. 2, 117 (1980).
25. V. F. Kositsyn and A. E. Konyaev, "Investigation of the effect of multiplication in spherical samples of fissionable materials," Preprint VNIINM P-8 (28), Moscow (1980).

A RELATIONSHIP BETWEEN THE NORMALIZED EQUIVALENT AND EXPOSURE DOSAGES OF PHOTON RADIATION

Yu. G. Kostyleva and I. P. Mysev

UDC 529.1.08:539.12:539.122

One of the possible ways of estimating in accordance with NRB-76 [1] the maximum equivalent dosage of photon radiation in a critical organ upon irradiation of the entire body is the use of a relationship between this quantity and the exposure dosage, which is most often measured in practice.

In NRB-76 an analogous relation is given for the flux of photons, which does not, however, have sufficiently wide application. In addition there are no indications of the conditions of its measurement – in free air or on the front surface of a skin-equivalent phantom in the presence of inversely scattered radiation. This relationship is given for the maximum possible equivalent (absorbed) dosage D_o under conditions of electron equilibrium without taking account of absorption of radiation in the layer shielding the critical organ, although the thickness of the layer for the individual organs is given in NRB-76 (see Table 1). The use of this relationship formally denotes that radiation monitoring is performed at some photon energy with account taken of the most rigorous requirement – the limiting permissible dosage LPD_I for critical organs of group I.

The contribution of inversely scattered radiation and the absorption of radiation are taken into account in the MÉK document [2] in the relationship between the dosage absorbed in air and the depth equivalent dosage by H_d – the dosage absorbed in a round phantom 30 cm in diameter at a depth t_d, which is considered as the upper limit of the effective equivalent dosage H_e. It has been indicated in this document that of the three normalized recommendations of MKRZ [3] of equivalent dosages (the dosage H_e, the dosage for the crystalline lens of the eye H_γ, and the dosage for the remaining organs, called the skin dosage H_s) the adopted relationships between the values LPD_i and t_i permit monitoring only two: H_d and H_s. Satisfaction of the norms for them automatically indicates satisfaction of the norm for H_γ as well, excluding the narrow range of photon energy $10 < E < 13$ keV, which one can neglect in the majority of cases. However, additional monitoring of H_γ should also be provided for upon a decrease of LPD_γ.

Thus the application of the existing relationships between the equivalent dosage and the various characteristics of the radiation field leads in NRB-76 to an overestimation of the irradiation for all three groups of critical organs and in the MÉK document – to the necessity of monitoring the depth absorbed dosages either at two depths in the phantom with preservation of the fundamental possibility of nonobservance of the norm for the dosage H_γ or at three depths.

Analysis of NRB-76 and the MÉK document shows that a development of their positions is possible which permits monitoring only one quantity – the normalized equivalent dosage H_M,

Translated from Atomnaya Énergiya, Vol. 57, No. 5, pp. 359-362, November, 1984. Original article submitted August 15, 1983.

0038-531X/84/5705-0791$08.50

TABLE 1. A Comparison of Criteria and Methods of Radiation Monitoring

Normalized dosage H_M	Limiting permissible dosage LPD_i and thickness t_i of the layer for the i-th group of critical organs or the depth t_i of the phantom for the i-th dosage being monitored			Method of monitoring the dosage H_M	Factor LPD_i/D in the H_M/X relationships
	Group I	Group II	Group III		
Maximum equivalent dosage in a critical organ (NRB-76)	LPD_I = 5 rems t_I = 5000 mg/cm² (red bone marrow) t_I = 500 mg/cm² (gonads) t_I = ? (whole body)	LPD_{II} = 15 rems t_{II} = 300 mg/cm² (crystalline lens of the eye) t_{II} = ? (remaining organs)	LPD_{III} = 30 rems t_{III} = 7 mg/cm² (skin) t_{III} = ? (remaining organs)	Monitoring of the maximum dosage D_0 with overestimation of the dosage: $D_0 < LPD_I < LPD_{II} < LPD_{III}$	1
Depth equivalent dosages at two or three* depths (MÉK) document)	Depth H_d (as the upper limit of the effective H_e) LPD_e = 5 rems t_d = 1000 mg/cm²	For the crystalline lens of the eye H_l LPD_l = 15 rems t_l = 300 mg/cm²	For the remaining organs H_s LPD_s = 50 rems t_s = 7 mg/cm²	Monitoring of the dosages H_e and H_s with two dosimeters having a risk of underestimation of the dosage H_l or monitoring of the dosages H_e, H_l, and H_s with three dosimeters: $D(1000) < LPD_e$ $D(300) < LPD_l$ $D(7) < LPD_s$	LPD_e/D_0 according to O_5AEL, LPD_l/D_0 according to $O_{15}ABFM$, and LPD_s/D_0 according to $O_{50}EFG$ (see Fig. 1)
Maximum equivalent dosage in a critical organ of any of the groups of NRB-76 or any equivalent dosage of the MÉK document (this paper)	Depth $H(t_I)$ $LPD_I = LPD_e$ = 5 rems $t_I = t_d$ = 1000 mg/cm²	Depth $H(t_{II})$ $LPD_{II} = LPD_l$ = 15 rems $t_{II} = t_l$ = 300 mg/cm²	Depth $H(t_{III})$ LPD_{III} = 300 rems or LPD_s = 50 rems $t_{III} = t_s$ = 7 mg/cm²	Monitoring of dosages at three depths with a single dosimeter: $D(1000) < LPD_I = LPD_s$ $D(300) < LPD_{II} = LPD_l$ $D(7) < LPD_{III}$ or LPD_s	LPD_I/D_M according to O_5ABC or O_5ABFG (see Figs. 1 and 2a)

*May be realized upon necessity.

Declassified and Approved For Release 2013/02/22 : CIA-RDP10-02196R000300050005-2

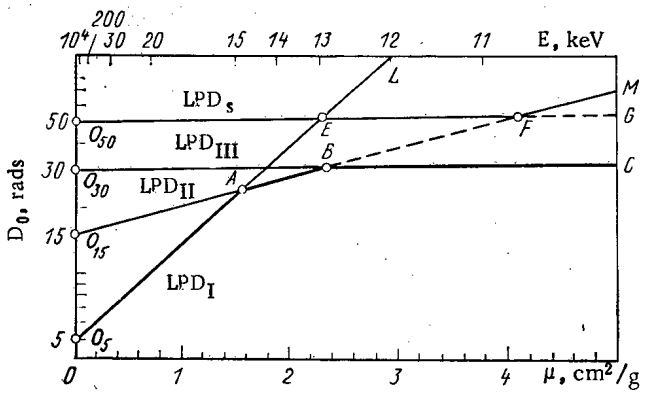

Fig. 1. Dependence of the absorbed dosage on the phantom surface D_o on the attenuation coefficient μ and the photon energy E for different cases (see Table 1). The envelopes of D_M O_5ABC are for the NRB-76 norms, and BFG is the noncoincident part for the MÉK document.

which is related to the exposure dosage X by the relationships $H_M/X = f(E)$, for which either the NRB-76 norms for a critical organ of any of the three groups with the additional assumption of the shielding layer thickness or the norm of the MKRB recommendations are satisfied for any of the dosages H_e, H_γ, and H_s with monitoring of the dosage H_e in accordance with the MÉK document.

In order to obtain the H_M/X relationships, we shall assume for simplicity's sake that the radiation is incident normally on a semiinfinite skin-equivalent phantom and the absorbed dosage declines exponentially as a function of phantom depth with the attenuation coefficient μ. We shall also assume that the thickness t_i of the layers shielding some organ of the i-th group of NRB-76 (or the depth t_i at which the i-th depth dosage is monitored in accordance with the MÉK document) is equal to the values indicated in Table 1, and we shall consider the families of straight lines (Fig. 1)

$$D_0(\mu) = \mathrm{LPD}_i \exp(\mu t_i),$$

which represent the maximum dosage D_o on the phantom surface on which the dosage at a depth t_i is equal to the corresponding LPD_i according to Table 1.

It is evident that in different intervals of μ normalization of the dosage D_o is based on the LPD of only one group of critical organs (or one depth dosage) in accordance with the shape of the broken lines — the envelopes $D_M(\mu)$ of the families of these straight lines. The shape of $D_M(\mu)$ depends on the values of LPD_i and t_i, coinciding for NRB-76 and the MÉK document at $E > 15$ keV and differing at lower energies due to disagreement between LPD_{III} and LPD_s. For NRB-76 and the adopted values of the shielding layer thickness the critical organs are those of group I for $E > 15$ keV, group II for $13 < E < 15$ keV, and group III for $E < 13$ keV. Similarly when normalizing the dosage in accordance with the MÉK document, the monitoring should be performed according to the dosage H_d for $E > 15$ keV, the dosage H_γ for $11 < E < 15$ keV, and the dosage H_s for $E < 11$ keV, which corresponds approximately to the estimates of this document.

We shall reorganize D_M in the form of a $LPD_I/D_M(E)$ dependence (Fig. 2a), and we shall switch from the dosage D_o [rads] to the exposure dosage X_R[P] measured in air on the front surface of the phantom with the help of the coefficient (Fig. 2b)*

$$k_X(\bar{E}) = D_0/X_R = 0{,}873\,\mu_t/\mu_a,$$

where μ_t/μ_a is the ratio of the true absorption coefficients for mouse tissue and air. We shall on this basis find the desired relationships between the dosages H_M and X_R (Fig. 2c):

$$H_M/X_R = [\mathrm{LPD}_I/D_M(E)]\,k_X(E).$$

*1 rad = 0.01 Gy; 1 P = 2.58×10^{-4} Kl/kg.

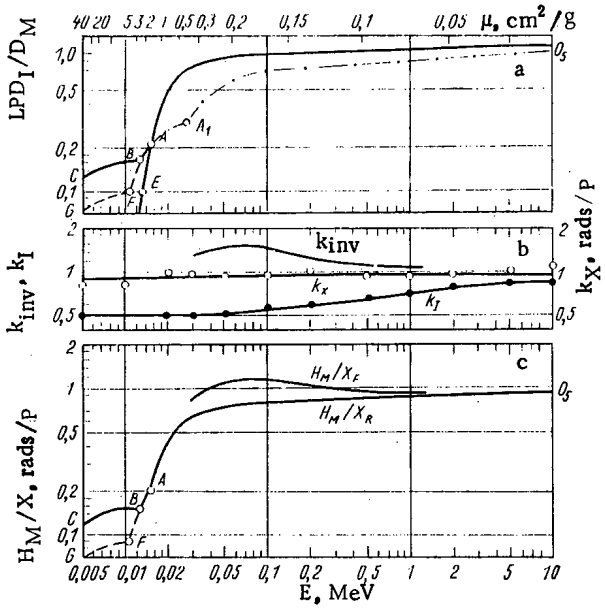

Fig. 2. Ratios between the normalized equivalent H_M and exposure X dosages and their components as a function of the energy E and the attenuation coefficient μ: a) the ratio LPD_I/D_M of the depth dosage to the dosage D_o with account taken of the relationships between LPD_i (—— — for the NRB-76 norms; - -- — noncoincident part for the MÉK document with estimation of H_e from H_d; and -. -.- — with account taken of H_e directly); b) coefficients of inverse scattering k_{inv} [4], anisotropy k_I (• — data of NRB-76), and the transition to dosage X, k_X (—— — calculations according to the data of [5] for E <10 keV and recalculation [6] for E ⩾10 keV; ○ — NRB-76 recalculation); and c) the ratios X_R and H_M/X_F upon the measurement of the dosage X accordingly on the front surface of the phantom and in free air (see the notation of Fig. 2a). The open circles of Figs. 2a and c correspond to Fig. 1.

In the case in which the exposure dosage in free air is measured — X_F, this expression should be multiplied by the coefficient of inverse scattering $k_{inv} > 1$ (see Fig. 2b), which is dependent on the dimensions of the radiation field and the phantom. For these conditions (see Fig. 2c)

$$H_м/X_F = [\Pi Д Д_I/D_м(E)]\, k_X(E)\, k_{inv}(E).$$

A similar curve for the dosage absorbed in air in the 0.015-4-MeV range is given in the MÉK document. It has the same kind of energy dependence as does the H_M/X_F curve.

The expressions obtained can be calculated in a similar fashion for a more accurate model of the phantom, for example, an anthropomorphic one, with refinement of the thickness t_i for NRB-76 or with account taken of the weighting factors of the different organs [3] and their distributions with depth upon consideration of the dosage H_e. Thus it is not obligatory in the calculation of H_M/X to estimate H_e from the dosage at a fixed depth. The replacement of H_d by H_e in accordance with the H_d/H_e curve of the MÉK document leads to a more abrupt decline of H_M/X as the energy decreases: up to a factor of 2.3 at an energy of 30 keV, to which the interval monitored from the dosage H_7 (point A_1 in Fig. 2a) has expanded. When the dosage H_d is kept as the estimate of H_e, this indicates the advisability of increasing the depth t_d to 2-3 g/cm², depending on the energy range being approximated on the basis of the shape of the H_d/H_e curve.

The following factors affect H_M/X to a lesser extent. A more accurate choice of the phantom shape and taking account of the accumulation factor, lead, as the analysis of [7] shows, to an increase of H_M/X on the sections O_5L and $O_{15}M$ (see Fig. 1) of no more than 10 and 6% respectively, for a phantom in the form of an infinite elliptical cyclinder with 24- and 36-cm axes. A change in the coefficient k_X due to the inversely scattered radiation, which has a softer spectrum than does the incident radiation, has practically no effect on H_M/X, since this coefficient varies by no more than ± 3% with respect to the average value of 0.93 rad/P over the entire energy range under discussion. Nonsatisfaction of electron equilibrium, which increases as E and the mean free path R of the secondary electrons increase, increases H_M/X by $\mu R/3$ [8] (3% at 10 MeV) due to an excess of the absorbed dosage in air over the energy equivalent dosage X on the one hand and decreases it by $\mu(R - t_I)$ at E > 2 MeV (9% at 10 MeV) on the other hand due to a shift of the maximum absorbed dosage within the phantom by a distance R when $R > t_I$ and the recorded radiation is free of electrons. To sum up, there is no understating of the dosage H_M for high-energy photons.

The H_M/X relationships obtained for unidirectional radiation can be recalculated for isotropic radiation in accordance with NRB-76 by multiplying it by the anisotropy coefficient $k_I < 1$ (see Fig. 2b). The coefficients k_{inv} and k_I can be refined only for the specific measurement conditions; in the general case their indeterminacy is very appreciable — up to a factor of 1.5 for k_{inv} and up to a factor of two for k_I. Taking account of the relatively low requirements on the accuracy with which the equivalent dosage is measured [9], refinement of the calculations of H_M/X, which are the upper limits of the dosage H_M under the adopted assumptions, seems premature prior to the refinement of the phantom model, which introduces the greatest indeterminacy.

The possibility of monitoring with a single dosimeter the NRB-76 norms or the MKRZ recommendations in actual fields of photon radiation is determined by the degree of agreement of the energy dependence of the dosimeter with the relationships obtained and the shape of the radiation spectrum. A more complicated method of monitoring with the use of several dosimeters, which measure the absorbed dosage at specified depths, permits, when necessary, establishing in addition the cause of the radiation overdosage (the critical organ group or the dosage being monitored), so that the final choice of method is determined by the problems and conditions of the monitoring. In order to estimate the dosage H_M by measuring the absorbed dosage at one or several depths t_d in the phantom similarly to Fig. 1 (upon maintenance of the boundaries of the energy intervals with predominance of monitoring according to this or the other LPD_i), a family of straight lines $D_d(\mu) = LPD_i \exp[\mu(t_i - t_d)]$ is constructed which permits, for example, selecting the optimal positions of t_d and the relationships between the dosimeter sensitivity.

We also note that this same approach is applicable to β radiation. With allowance for the assumption of an exponential nature of the radiation attenuation, the coefficients μ at the points A, B, and F (see Fig. 1) correspond to a rather large maximum energy of the β spectrum: 4.3 MeV for NRB-76 (point B), 2.4 MeV for the MKRZ recommendations (point F), and over 5 MeV (point A).

The combined measurements of the dosages which form the basis of the calculation of H_M/X, which correspond in the case of the MKRZ recommendations to phenomena of a different nature having a threshold-free stochastic or a threshold dependence on the dosage, are evidently legitimate if the monitoring of H_M is performed only in order to ascertain that the regulated norms are observed.

With calibration of the dosimeters the choice of this or another H_M/X relationship is determined by the recording of inversely scattered radiation under working conditions: H_M/X_R is used for individual dosimeters, and H_M/X_F is used for the so-called inspection dosimeters. The exposure dosage is measured under the conditions in which the calibration is performed. In order to raise the accuracy of the calibration, it is advisable to use a phantom which corresponds to the measurement conditions. It is necessary both in the calibration and the measurements to satisfy the conditions of electron equilibrium, which is attained primarily by the choice of a sufficiently large thickness of the front wall of the detector, which should exceed the mean free path R of the secondary electrons, or by the application of an additional air-equivalent filter of deficient thickness. In the opposite case if this condition is satisfied during calibration but is not satisfied during the measurements, the dosimeter will understate the dosage, or vice versa. Upon calibration in the radiation field of x-ray apparatuses or electron accelerators the H_M/X relationships are averaged over the

dosage spectrum of the radiation, using the additivity property of the dosage H_M, and the exposure dosage at high energy is determined by the method of indirect measurement with the help of dosimeters of the transport of bremsstrahlung energy.

The relationships obtained can be used as correction factors to the readings of operating exposure-dosage dosimeters (from the standpoint of energy dependence many industrial dosimeters have turned out to be applicable for an even wider energy range), as the recommended calibration characteristics in the development of dosimeters of normalized equivalent dosage, and in the calibration of radiation monitoring dosimeters directly in units of the limiting permissible dosage LPD or the permissible dosage strength PDS.

The authors express their gratitude to V. V. Matveev and A. D. Sokolov for interesting discussions and valuable remarks.

LITERATURE CITED

1. NRB-76 Norms of Radiation Safety [in Russian], Énergoizdat, Moscow (1981).
2. "Beta, X, and γ radiation dose equivalent and dose equivalent rate meters for use in radiation protection," IEC Document 45B (Central Office) 43, Technical Committee No. 45, February 1982.
3. Radiation Protection. MKRZ Recommendations [in Russian], Publication 26, Atomizdat, Moscow (1978); Limits of Entry of Radionuclides for Those Working with Ionizing Radiation. MKRZ Recommendations [in Russian], Publication 30, Part I, Énergoizdat, Moscow (1982).
4. Radiation Dosimeters [Russian translation], IL, Moscow (1958), p. 453.
5. É. Storm and Kh. Israél', Interaction Cross Sections of Gamma Radiation [Russian translation], Atomizdat, Moscow (1973).
6. Physical Aspects of Irradiation, ICRU Report 10b (1962).
7. V. L. Gozenbuk et al., Dosage Load on a Person in Gamma-Neutron Radiation Fields [in Russian], Atomizdat, Moscow (1978).
8. Yu. G. Kostyleva and I. P. Mysev, in: Advances in Physical and Biological Radiation Detectors, IAEA-SM-143/67, IAEA, Vienna (1971).
9. "Radiation safety — quantities, units, methods, and devices," Reports 19 and 20 of MKRE [in Russian], Atomizdat, Moscow (1974).

KINETIC FUNCTIONS OF THE DELAYED NEUTRONS FROM A MIXTURE OF THE NUCLIDES ^{232}Th AND ^{238}U

P. P. Ganich, M. V. Goshovskii, A. I. Lendel,
V. I. Lomonosov, D. I. Sikora, and S. I. Sychev

UDC 539.173.3

In [1], Keepin proposed a method for the determination of the content of fissile nuclides in multicomponent mixtures, for example ores, fresh and spent fuel, by means of kinetic functions describing the emission of delayed neutrons during the irradiation with neutrons of the samples being investigated. In [2, 3], Keepin's method was used for the analysis of fissile nuclides in electron accelerators using as its basis the emission of delayed neutrons as a result of photofission.

The analysis of the fissile nuclides in electron accelerators by G. Keepin's method is characterized by the simplicity, economy and low level of activation of fissile nuclides in the samples. However, its application for the analysis of certain pairs of fissile nuclides in mixtures is restricted because of the small descrimination ratios of the kinetic functions.

The kinetic functions, the number of delayed nuetrons in which is normalized to the yield of γ-quanta of the nucleus-fission fragment ^{133}I, are characterized by large discrimination ratios [4]. Therefore, in order to develop the method of [4], it will be of interest to what extent they can be used for the determination of the content of fissile nuclides in two-component mixtures, and what are their advantages by comparison with G. Keepin's kinetic functions. In connection with this, the analysis of a mixture of ^{232}Th + ^{238}U was conducted on the M-30 microtron by two methods of normalizing the number of delayed neutrons in the kinetic functions: to the total yield of delayed neutrons and to the yield of ^{133}I γ-quanta.

In the general case [1], in order to determine the content of fissile nuclides in a mixture, a set of experimental values of the kinetic functions alone is insufficient. Actually, from the interrelation between the kinetic functions of individual nuclides S_1, S_2....S_n, of the mixture S_m and the yields of fission products or their radiations Y_1, Y_2, ...Y_n, in which the number of delayed neutrons is normalized,

$$S_m = \frac{\sum_{l=1}^{n} \alpha_{l1} S_l}{\sum_{l=1}^{n} \alpha_{l1}}; \qquad \alpha_{l1} = \frac{C_l Y_l}{C_f Y_1}, \tag{1}$$

transforming with the condition $\sum_{l=1}^{n} C_l = 1$ to the form

$$\sum_{l=2}^{n} \left(1 + \frac{Y_l}{Y_1} \frac{D_{lm}-1}{D_{m1}-1} D_{m1}\right) C_l = 1 \tag{2}$$

($D_{lm} = S_l/S_m$ is the discrimination ratio of the kinetic functions) it follows that in order to determine the relative concentrations of fissile nuclides in the mixture C_l, in addition to the values of the kinetic functions $S_r = S_r^+(f,Y)$ or $S_r = R_r^+(f,Y)$, it is necessary to know also the experimental values of the ratios of the yields Y_l/Y_1: with G. Keepin's set of kinetic functions — the ratio of the total yields of delayed neutrons, and with the set of kinetic functions of [4] — the ratio of the γ-quanta yields of ^{133}I. The ratios of the yields Y_l/Y_1 can be determined most simply from expression (2) by using the kinetic functions of two-component mixtures with known content of fissile nuclides. Thus, the procedure for carrying out the analysis of two-component mixtures, in addition to the independent use, is of interest for finding the ratios Y_l/Y_1.

Translated from Atomnaya Énergiya, Vol. 57, No. 5, pp. 363-364, November, 1984. Original article submitted May 10, 1983.

0038-531X/84/5705-0797$08.50

TABLE 1. Average Values of the Relative Concentration C_U

Mixture No.	Starting data	$S_r^+(f, Y)$	$R_r^+(f, Y)$	$S_r^{+\Delta}(f)$
2	0,697	0,753±0,055	0,772±0,071	0,774±0,191
3	0,458	0,408±0,021	0,380±0,024	0,545±0,068
4	0,174	0,153±0,023	0,147±0,022	0,209±0,068

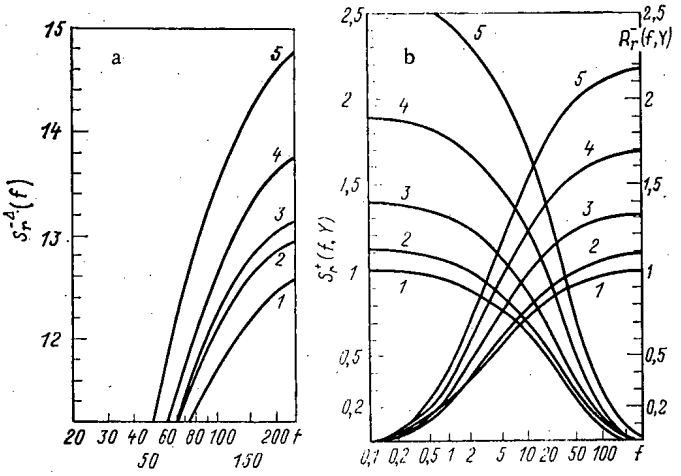

Fig. 1. Kinetic functions $S_r^{-\Delta}(f)$ (a), $R_f^+(Y)$ and $S_f^+(Y)$ (b); 1) ^{238}U; 2) mixture 2; 3) mixture 3; 4) mixture 4; 5) ^{232}Th.

The composition of the two-component mixture was determined by the authors of this paper in the following way. Fresh samples, containing ThO_2, U_3O_8 and their mixture, were irradiated in the M-30 microtron with bremsstrahlung radiation with an energy of the accelerated electrons of 15.5 MeV and an average current of 9 μA. The maximum energy of the bremsstrahlung radiation was chosen lower than the threshold energy of the reaction $^{18}O(\gamma, p)^{17}N$ for the purpose of excluding delayed neutrons from ^{17}N nuclei. The time distribution of the delayed neutrons and the yield of γ-quanta from the ^{133}I fission fragments were measured by the procedures described in [3, 4].

The total yields of delayed neutrons and the ^{133}I γ-quanta yields from samples of uranium $Y_2 \equiv Y_U$ and thorium $Y_1 \equiv Y_{Th}$, were measured directly on the M-30 microtron with monitoring of the bremsstrahlung radiation passing through the ionization chamber. Their ratios are equal to $Y_U/T_{Th} = 2.20 \pm 0.09$ with G. Keepin's set of kinetic functions, and $Y_U/Y_{Th} = 4.47 \pm 0.02$ with the set of kinetic functions from [4]. The mass of the samples amounted to ∿6 g.

In order to determine the kinetic functions which are shown in Fig. 1, the time distributions of the delayed neutron pulses were used, the maximum number of which for different samples amounted to $(1.7 - 3.0) \cdot 10^4$, and the ^{133}I γ-quanta yields were measured with an accuracy of 3 - 5%.

The relative concentration of ^{238}U was determined directly from condition (2) for each value of f in the interval 0.6-2 sec.

Table 1 shows the average values of the relative concentration C_U, their errors for three mixtures using the values of the kinetic functions $S_r^+(f,Y)$, $R^+(f,Y)$ [4], and $S_r^{+\Delta}(f)$ [1] in expression (2). It follows from the table that on the M-30 microtron the content of fissile nuclides in fresh two-component mixtures can be determined by the above-described procedure, with errors of $\Delta C_U \approx 0.06$ and $\Delta C_U \approx 0.2$ by using the values of the kinetic functions $R_r^+(f,Y)$ and $S_r^+(f,Y)$ from [4] and $S_r^{+\Delta}(f)$ from [1] respectively, where $r = l$, m.

In conclusion, we note that a reduction of the errors in determining the content of fissile nuclides in a two-component mixture is attainable by normalizing the delayed neutrons to the ^{133}I γ-quanta yield.

The authors thank A. M. Parlag and K. D. Popovich for valuable discussion and assistance in the task.

LITERATURE CITED

1. G. Keepin, "Nondestructive detection, identification and analysis of fissionable materials," in: Proceedings of a Symposium on Safeguards Research and Development, 1079 USAEC, Washington (1967), p. 150.
2. M. M. Dorosh, N. I. Kovalenko, A. M. Parlag, and V. A. Shkoda-Ul'yanov, "Investigation of the feasibility of using Keepin's method for the separate determination of fissile elements in mixtures, using a beam of gamma-quanta," At. Énerg., 35, No. 1, 59-61 (1973).
3. B. M. Aleksandrov, P. P. Ganich, A. S. Krivokhatskii, et al, "Determination of the kinetic functions of delayed neutrons from the photofission of heavy isotopes," At. Énerg. 44, No. 6, 526-528 (1978).
4. P. P. Ganich, A. S. Krivokhatskii, A. I. Lendel, et al., "On the complex use of delayed neutrons and photofission γ-quanta for the identification of fissile nuclides," At. Énerg., 55, No. 4, 247-249 (1983).

RADIOELECTROCHEMICAL CONVERSION OF THE ENERGY OF IONIZING RADIATION IN A CELL WITH A SEMICONDUCTING ELECTRODE

M. D. Krotova, A. A. Revina, Yu. V. Pleskov, A. M. Morozov, G. E. Zakharov, T. B. Ashrapov, and É. F. Kalinichenko

UDC 621.039.667:533.9.082.89

In [1-3] the fundamental possibility of converting the energy of ionizing radiation into the chemical energy of hydrogen in an electrochemical cell with a semiconducting electrode is demonstrated and the laws governing this process are studied. The principle of the method is very similar to the principle of photoelectric conversion of light energy [4]. The absorption of the energy of the ionizing radiation in the semiconductor is accopanied by generation of nonequilibrium electron–hole pairs [5]; in addition, the minority carriers move under the action of the electric field toward the electrode/electrolyte interface, while the majority carriers move into the bulk of the semiconductor and are then transferred along the external ciruit to the auxiliary (metallic) electrode of the electrochemical cell. The appearance of nonequilibrium carriers at the electrode/electrolyte interfaces stimulates the flow of electrochemical reactions. In water solutions of electrochemically inactive electrolytes, this is the liberation of hydrogen at the cathode and oxygen at the anode.

Thus, the electrolytic decomposition of water occurs is a result of the absorption of the energy of the ionizing radiation in the semiconductor and the rate of this reaction can be monitored by measuring the electrical current in the circuit of the cell at the moment the radiation acts.

It was of interest to study the radioelectrochemical decomposition of water induced under real conditions by the radiation from the BBP-SM reactor at the Institute of Nuclear Physics of the Academy of Sciences of the Uzbek SSR. In these experiments, we measured the radioelectrochemical current in a cell with a semiconducting electrode and a metallic cathode.

The cell consisted of a cylindrical stainless steel vessel with a diameter of 25 mm and a height of 300 mm. The cathode was a cylinder made of nickel sheet metal. We fastened the anode to a sealed input lead, situated on the cover of the cell and insulated electrically from the housing. A thermocouple was attached to the anode input in order to measure the temperature in the cell. Tubes for injecting the solution and removing the liberated gases were also placed on the cover. We placed the cell in one of the channels of the reactor, intended for physicochemical experiments. Due to the cooling of the cell by water, the temperature of the irradiated electrolyte did not exceed 75°C. At the location of the cell in the 10-MW reactor, the fast-neutron flux density (varying somewhat along the electrode) was equal to $(1.2\text{-}2.4)\times10^{13}\,\text{cm}^{-2}\cdot\text{sec}^{-1}$ for energies > 1.15 MeV; $(0.58\text{-}1.11)\cdot10^{13}\,\text{cm}^{-2}\cdot\text{sec}^{-1}$ for energies > 2.3 Mev; $(3.1\text{-}6.0)\cdot10^{11}\,\text{cm}^{-2}\cdot\text{sec}^{-1}$ for energies > 5 MeV; and $(3.1\text{-}6.1)\cdot10^{13}\,\text{cm}^{-2}\cdot\text{sec}^{-1}$ for thermal neutrons.

The semiconducting anodes were prepared at the A. N. Frumkin Institute of Electrochemistry of the Academy of Sciences of the USSR. We deposited the electrochemically active semiconductor TiO_2 in the form of a film ("smooth electrode") or a porous mass on a titanium sheet-metal substrate (a plate 210 mm long and 16 mm wide) by means of thermal oxidation of titanium [2]. The porous anode consisted of a ceramic mass (composition: TiO_2 and an atomic fraction of Nb_2O_5 0.001%), deposited on the substrate and anealed in hydrogen.

We performed the electrochemical measurements in a 1 N alkali solution (KOH, LiOH). We obtained the polarization curves with the help of a P 5848 potentiostat using a two-electrode scheme. In order to stabilizae the potential of the nickel cathode, prior to the experiment we treated the cathode so as to saturate it with hydrogen, after which the potential was equal to -0.96 ± 0.1 V (with respect to the saturated clorine-silver electrode), which is close to the potential of a reversible hydrogen electrode. The electrolyte level in the cell corresponded to the visible surface of the immersed part of the anode $\sim 50\,\text{cm}^2$. The volume of the solution in the cell was $\sim$100 ml.

Translated from Atomnaya Énergiya, Vol. 57, No. 5, pp. 364-365, November, 1984. Original article submitted January 3, 1983; revision submitted June 21, 1984.

 0038-531X/84/5705-0800$08.50

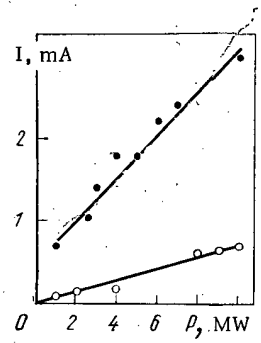

Fig. 1

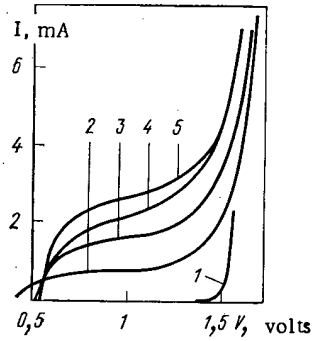

Fig. 2

Fig. 1. Dependence of the cell current on the reactor power for a porous (●) and a smooth (◎) electrode.

Fig. 2. Polarization curves of the cell with a porous electrode. The reactor power was equal to 0, 1, 3, 5, and 7 MW (1-5), and the temperature of the cell for 2-5 was 25, 58, 68, and 72°C, respectively.

Results and Discussion. We determined the rate of the radioelectrochemical decomposition of water by measuring the current in the cell as a function of the potential of the electrode, the power of the reactor, and time. Measurements outside the reactor (in the dark) showed that with a voltage of less than 1 V the current in the cell is negligibly small. In the reactor, the cell current varies proportonally to the reactor power (Fig. 1); in addition, the current is several times higher for the porous anode than for the smooth anode. The dependence of the current on the voltage on the cell (polarization curve, Fig. 2) has practically the same form for both the smooth and porous electrodes and is qualitatively similar to the form observed when a titanium-oxide anode is irradiated by accelerated electrons [2] or ultraviolet radiaton.

The curves presented indicate that the nature of the observed acceleration of the electrochemical reaction under irradiation in a reactor is the same as under conditions of the model irradiation [1-3], i.e., the generation of nonequilibrium current carriers in the semiconductor lies at the foundation of this acceleration. The cell current at first drops noticeably, and the stabilizes. Under irradiation in a reactor for 1000 h, the current decreased by approximately a factor of two.

The rate of the radioelectrochemical decomposition of water, determined by measuring the electrical current, was approximately 100 times lower than the rate of the simultaneously occurring radiolysis of water in the cell, as determined from the liberation of gas (the efficiency of the radioelectrochemical process $\sim 0.005\%$). The low conversion efficiency is explained [2, 3] by the fact that only an insifnifcant fraction of the radiation is absorbed in the region of the space charge of the semiconductor. The presence of an extended surface increased the efficiency of energy conversion when a porous electrode was used. Since the conditions of the radioelectrochemical process were not optimized, there are grounds for believing that the decomposition of water can be substantially improved by increasing the semiconductor/solution mass ratio as well as by improving the structure and composition of the semiconducting electrode.

LITERATURE CITED

1. Yu. V. Pleskov, M. D. Krotova, and A. A. Revina, Inventor's Certificate No. 807672, Byull. Izobret., No. 43 (1982).
2. M. D. Krotova, Yu. V. Pleskov, and A. A. Revina, Elektrokhimiya, 17, No. 4, 528-533 (1981).
3. M. D. Krotova, Yu. V. Pleskov, A. A. Revina, and V. A. Ryadovskii, ibid., 19, No. 3, 351-355 (1983).
4. Yu. V. Pleskov, ibid., 17, No. 1, 3-31 (1981).
5. V. I. Veselovskii, in: International Geneva Conference on the Global Use of Atomic Energy [in Russian], Vol. 7, Atomizdat, Moscow (1955), pp. 727-734.

How To Comply With The New Copyright Law

Participation in the Copyright Clearance Center (CCC) assures you of legal photocopying at the moment of need.

Libraries everywhere have found the easy way to fill photocopy requests legally and instantly, without the need to seek permissions, from more than 3000 key publications in business, science, humanities, and social science. You can:

Fill requests for multiple copies, interlibrary loan (beyond the CONTU guidelines), and reserve desk without fear of copyright infringement.

Supply copies from CCC-registered publications simply and easily.

The Copyright Clearance Center is your one-stop place for on-the-spot clearance to photocopy for internal use.

Its flexible reporting system accepts photocopying reports and returns an itemized invoice. You send only one convenient payment. CCC distributes it to the many publishers whose works you need.

And, you need not keep any records, the CCC computer will do it for you. Register now with the CCC and you will never again have to decline a photocopy request or wonder about compliance with the law for any publication participating in the CCC.

To register or for more information, just contact:

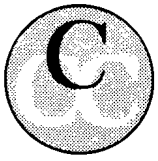

Copyright Clearance Center
21 Congress Street
Salem, Massachusetts 01970
(617) 744-3350

a not-for-profit corporation

NAME _____ TITLE _____

ORGANIZATION _____

ADDRESS _____

CITY _____ STATE _____ ZIP _____

COUNTRY _____ TELEPHONE _____

CHANGING YOUR ADDRESS?

In order to receive your journal without interruption, please complete this change of address notice and forward to the Publisher, 60 days in advance, if possible.

(Please Print)

Old Address:

name _____

_____

address _____

city _____

state (or country) _____ zip code _____

New Address

name _____

_____

address _____

city _____

state (or country) _____ zip code _____

date new address effective _____

name of journal _____

THE LANGUAGE OF SCIENCE
Plenum
PUBLISHING CORPORATION

233 Spring Street, New York, New York 10013

MEASUREMENT TECHNIQUES
Izmeritel'naya Tekhnika
Vol. 27, 1984 (12 issues) $520

MECHANICS OF COMPOSITE MATERIALS
Mekhanika Kompozitnykh Materialov
Vol. 20, 1984 (6 issues) $430

METAL SCIENCE AND HEAT TREATMENT
Metallovedenie i Termicheskaya Obrabotka Metallov
Vol. 26, 1984 (12 issues) $540

METALLURGIST
Metallurg
Vol. 28, 1984 (12 issues) $555

PROBLEMS OF INFORMATION TRANSMISSION
Problemy Peredachi Informatsii
Vol. 20, 1984 (4 issues) $420

PROGRAMMING AND COMPUTER SOFTWARE
Programmirovanie
Vol. 10, 1984 (6 issues) $175

PROTECTION OF METALS
Zashchita Metallov
Vol. 20, 1984 (6 issues) $480

RADIOPHYSICS AND QUANTUM ELECTRONICS
Izvestiya Vysshikh Uchebnykh Zavedenii, Radiofizika
Vol. 27, 1984 (12 issues) $520

REFRACTORIES
Ogneupory
Vol. 25, 1984 (12 issues) $480

SIBERIAN MATHEMATICAL JOURNAL
Sibirskii Matematicheskii Zhurnal
Vol. 25, 1984 (6 issues) $625

SOIL MECHANICS AND FOUNDATION ENGINEERING
Osnovaniya, Fundamenty i Mekhanika Gruntov
Vol. 21, 1984 (6 issues) $500

SOLAR SYSTEM RESEARCH
Astronomicheskii Vestnik
Vol. 18, 1984 (6 issues) $365

SOVIET APPLIED MECHANICS
Prikladnaya Mekhanika
Vol. 20, 1984 (12 issues) $520

SOVIET ATOMIC ENERGY
Atomnaya Énergiya
Vols. 56-57, 1984 (12 issues) $560

SOVIET JOURNAL OF GLASS PHYSICS AND CHEMISTRY
Fizika i Khimiya Stekla
Vol. 10, 1984 (6 issues) $235

SOVIET JOURNAL OF NONDESTRUCTIVE TESTING
Defektoskopiya
Vol. 20, 1984 (12 issues) $615

SOVIET MATERIALS SCIENCE
Fiziko-khimicheskaya Mekhanika Materialov
Vol. 20, 1984 (6 issues) $445

SOVIET MICROELECTRONICS
Mikroélektronika
Vol. 13, 1984 (6 issues) $255

SOVIET MINING SCIENCE
Fiziko-tekhnicheskie Problemy Razrabotki Poleznykh Iskopaemykh
Vol. 20, 1984 (6 issues) $540

SOVIET PHYSICS JOURNAL
Izvestiya Vysshikh Uchebnykh Zavedenii, Fizika
Vol. 27, 1984 (12 issues) $520

SOVIET POWDER METALLURGY AND METAL CERAMICS
Poroshkovaya Metallurgiya
Vol. 23, 1984 (12 issues) $555

STRENGTH OF MATERIALS
Problemy Prochnosti
Vol. 16, 1984 (12 issues) $625

THEORETICAL AND MATHEMATICAL PHYSICS
Teoreticheskaya i Matematicheskaya Fizika
Vol. 58-61, 1984 (12 issues) $500

UKRAINIAN MATHEMATICAL JOURNAL
Ukrainskii Matematicheskii Zhurnal
Vol. 36, 1984 (6 issues) $500

Send for Your Free Examination Copy

Plenum Publishing Corporation, 233 Spring St., New York, N.Y. 10013
In United Kingdom: 88/90 Middlesex St., London E1 7EZ, England
Prices slightly higher outside the U.S. Prices subject to change without notice.

RUSSIAN JOURNALS IN THE PHYSICAL AND MATHEMATICAL SCIENCES

AVAILABLE IN ENGLISH TRANSLATION

ALGEBRA AND LOGIC
Algebra i Logika
Vol. 23, 1984 (6 issues) $360

ASTROPHYSICS
Astrofizika
Vol. 20, 1984 (4 issues) $420

AUTOMATION AND REMOTE CONTROL
Avtomatika i Telemekhanika
Vol. 45, 1984 (24 issues) $625

COMBUSTION, EXPLOSION, AND SHOCK WAVES
Fizika Goreniya i Vzryva
Vol. 20, 1984 (6 issues) $445

COSMIC RESEARCH
Kosmicheskie Issledovaniya
Vol. 22, 1984 (6 issues) $545

CYBERNETICS
Kibernetika
Vol. 20, 1984 (6 issues) $445

DIFFERENTIAL EQUATIONS
Differentsial'nye Uravneniya
Vol. 20, 1984 (12 issues) $505

DOKLADY BIOPHYSICS
Doklady Akademii Nauk SSSR
Vols. 274-279, 1984 (2 issues) $145

FLUID DYNAMICS
Izvestiya Akademii Nauk SSSR, Mekhanika Zhidkosti i Gaza
Vol. 19, 1984 (6 issues) $500

FUNCTIONAL ANALYSIS AND ITS APPLICATIONS
Funktsional'nyi Analiz i Ego Prilozheniya
Vol. 18, 1984 (4 issues) $410

GLASS AND CERAMICS
Steklo i Keramika
Vol. 41, 1984 (6 issues) $590

HIGH TEMPERATURE
Teplofizika Vysokikh Temperatur
Vol. 22, 1984 (6 issues) $520

HYDROTECHNICAL CONSTRUCTION
Gidrotekhnicheskoe Stroitel'stvo
Vol. 18, 1984 (12 issues) $385

INDUSTRIAL LABORATORY
Zavodskaya Laboratoriya
Vol. 50, 1984 (12 issues) $520

INSTRUMENTS AND EXPERIMENTAL TECHNIQUES
Pribory i Tekhnika Eksperimenta
Vol. 27, 1984 (12 issues) $590

JOURNAL OF APPLIED MECHANICS AND TECHNICAL PHYSICS
Zhurnal Prikladnoi Mekhaniki i Tekhnicheskoi Fiziki
Vol. 25, 1984 (6 issues) $540

JOURNAL OF APPLIED SPECTROSCOPY
Zhurnal Prikladnoi Spektroskopii
Vols. 40-41, 1984 (12 issues) $540

JOURNAL OF ENGINEERING PHYSICS
Inzhenerno-fizicheskii Zhurnal
Vols. 46-47, 1984 (12 issues) $540

JOURNAL OF SOVIET LASER RESEARCH
A translation of articles based on the best Soviet research in the field of lasers
Vol. 5, 1984 (6 issues) $180

JOURNAL OF SOVIET MATHEMATICS
A translation of Itogi Nauki i Tekhniki and *Zapiski Nauchnykh Seminarov Leningradskogo Otdeleniya Matematicheskogo Instituta im. V. A. Steklova AN SSSR*
Vols. 24-27, 1984 (24 issues) $1035

LITHOLOGY AND MINERAL RESOURCES
Litologiya i Poleznye Iskopaemye
Vol. 19, 1984 (6 issues) $540

LITHUANIAN MATHEMATICAL JOURNAL
Litovskii Matematicheskii Sbornik
Vol. 24, 1984 (4 issues) $255

MAGNETOHYDRODYNAMICS
Magnitnaya Gidrodinamika
Vol. 20, 1984 (4 issues) $415

MATHEMATICAL NOTES
Matematicheskie Zametki
Vols. 35-36, 1984 (12 issues) $520

continued on inside back cover